COMPARISON BETWEEN SMPS, NANO-SMPS AND EPIPHANIOMETER DATA AT AN URBAN BACKGROUND SITE (BLOOMSBURY) AND A ROADSIDE SITE (MARYLEBONE ROAD)

AURELIE CHARRON AND ROY M. HARRISON

Division of Environmental Health & Risk Management
School of Geography, Earth & Environmental Sciences
The University of Birmingham
Edgbaston, Birmingham B15 2tt
United Kingdom

Report to DEFRA prepared by the University of Birmingham and Casella Stanger under contract EPG 1/3/184 "Monitoring of Airborne Particulate Concentrations and Numbers in the UK".

Contents List

SUMMARY

- SMPS and nano-SMPS data (integrated particle number and particle number size distribution) have been compared at an urban background (Bloomsbury) and a roadside site (Marylebone Road) in London. An excellent agreement is found for particle numbers above 100 nm at the urban background site. The Scanning Mobility Particle Sizer (SMPS) measures lower particle numbers than the nano Scanning Mobility Particle Sizer (nano SMPS) at size diameters below 100 nm. The lower the particle diameter, the higher the divergence. Both lower efficiencies of the 3022A Condensation Particle Counter (SMPS) for smaller particles and larger losses by Brownian diffusion and diffusional broadening of small particles by the long 3071A Differential Mobility Analyser (SMPS) could explain this result since size-dependent lower efficiencies and losses are not corrected by the SMPS software. The excellent correlations for linear relationships between SMPS and nano SMPS data for particle size diameters below 100 nm could lead to the establishment of corrections of SMPS data.

- During the intercomparison, SMPS data at Marylebone Road were 10 times lower than the nano SMPS data (and 10 times lower than "historic" SMPS data measured at Marylebone Road). Nevertheless, excellent linear relationships are found between the two datasets. Such relationships might be used to correct SMPS data. Remarkably, an accurate tenfold factor seems to be a good correction factor, but currrently remains unexplained.

- At both sites particle number size distributions show a large dominant mode around 25 nm and another mode between 50 and 90 nm that is merged in the first one. Particle numbers increase at diameters below 7 nm. The first two modes are consistent with numerous published studies; but no mode is normally observed below 7 nm except in the case of new particle formation. At the time of the writing of this report, the increasing numbers of particles below 7 nm are considered as a measurement artefact and these particles are not examined further.

- The relative significance of particles in the 7-11 nm size range in contributing to the total atmospheric numbers at Bloomsbury and Marylebone Road are examined using nano SMPS data (size diameter range: 5-184 nm). At both sites, 7-11 nm particles represent in average 5% of total particle numbers measured by the nano SMPS.

- Results showed discrepancies between epiphaniometer data and surfaces calculated from SMPS measurements. Nevertheless, power relationships well fit the relationships between computed surfaces and the epiphaniometer surface at the two sites. Amazingly, the calculation of the "more sophisticated" Fuchs and active surfaces does not improve the fitted relationships. On the other hand, two different methods to assess the epiphaniometer surface from SMPS measurements have been compared. An almost constant factor 5 is found between these two different methods. At the time of writing of this report, we do not know the reasons of these discrepancies, but the good correlations suggest a calibration problem with at least one of the instruments and also possibly problems with at least one equation.

- As a result of common influential sources and common dispersion processes, significant correlations are found between the three particle metrics (number, surface, mass) and between the three particle metrics and gas phase measures of traffic pollution (except for Bloomsbury daily averages because of the small dataset). However, relationships using hourly values are too scattered to properly model particle surface or particle number from other measures. On the contrary, relationships using daily values lead to well defined relationships, especially with NOx. The use of the relationships presented in this report requires the exclusion of possible calibration problems with the instruments. However, results are promising.

- Some results presented in this report are provisional. They depend on the confirmation of SMPS, nano SMPS and epiphaniometer data and equations used to compute the active aerosol surface.

1. BACKGROUND AND OBJECTIVES

Many studies have related particulate matter to adverse effects on health but it is still unclear which particle metric or component has the most significant health effects. Recent epidemiological studies have shown that adverse health effects associated to airborne particles may be better correlated with metrics such as particle number or particle surface than particle mass (Donaldson et al., 1998 ; Maynard and Maynard, 2002). A number of toxicological studies have demonstrated that ultrafine particles of a material are more toxic than the same mass of fine particles of the same material (Oberdorster, 2000 ; Donaldson et al., 1998 and their references). The particle surface area might possibly be a key metric. Substances that are on the surface of particles (e.g. transition metals) are the chemical species that most readily interact with biological systems. Recent studies have shown that inflammation and lung tumours were correlated with particle surface area (Donaldson et al., 1998). However, current air quality standards are based on particle mass concentration (mostly PM_{10}). As a consequence PM_{10} concentrations and sometimes $PM_{2.5}$ concentrations are currently continuously measured while little information is available on particle number or particle surface area.

Ultrafine particles constitute a small part of the overall particulate mass of the aerosol but are present in very high numbers and contribute a significant part of the surface of the aerosol. As a consequence, some field studies have shown that particle numbers do not correlate well with particle mass (e.g. Tuch et al., 1997 ; Keywood et al., 1999 ; Molnár et al, 2002). Harrison et al. (1999) have found a significant linear relationship between PM_{10} and particle numbers at an urban background site in Birmingham. However, they have found strong deviations from this linear relationship during an episode of high PM_{10} concentrations due to fireworks and bonfires. Such a result suggests that when the dominant source is changed, the relationship between number and mass is changed. Morawska et al. (1999) have demonstrated that the poor relationship between TEOM and SMPS data even when SMPS data are converted to mass concentrations using an average density is the consequence of aerosols of different sizes and densities arising from a complex mixtures of different sources. All these findings suggest that particle mass cannot be used as a reliable surrogate for ultrafine particles in epidemiological studies.

Simultaneous measurements of particle size distributions using a Scanning Mobility Particle Sizer (SMPS) and a nano Scanning Mobility Particle Sizer (nano SMPS) and active surface using an epiphaniometer have been made during short field campaigns at a roadside site (Marylebone Road) and an urban background site (Bloomsbury) in London. Two SMPS have been continuously installed since 1998 at Marylebone Road and Bloomsbury; whilst the nanoSMPS is the property of the University of Birmingham and the epiphaniometer was supplied on loan by Matter Engineering (Switzerland). The current configuration of the Scanning Mobility Particle Sizers installed at Marylebone Road and Bloomsbury limits the minimum size of particles counted to 11 nm. The nano SMPS (nanoclassifier Model 3080N and ultrafine particle counter (TSI Model 3025) allow the assessment of particles below 11 nm.

These two campaigns will lead:

(1) to the comparison between the SMPS/nano SMPS data and then,

(2) to the assessment of particles of diameters below 11 nm that are not continuously measured at Bloomsbury and Marylebone Road,

(3) to the comparison between the active surface of the aerosol from the epiphaniometer and surfaces derived from SMPS measurements,

(4) the comparison between the 3 particle metrics (number, surface, mass) and gas phase measures of traffic pollution in order to establish surrogate relationships that might be used for epidemiological studies.

Some results and interpretation in this report are provisional depending on confirmation of data (any calibration problem should be resolved) and/or equations used to compute specific aerosol surfaces.

2. SAMPLING SITES AND INSTRUMENTS

2.1 Sampling Sites

London Bloomsbury

This site is located within the south east corner of Russell Square Gardens in central London, generally laid to grass but with many mature trees. All four sides of the gardens are surrounded by a busy 2/4 lane one-way road system carrying approximately 35,000 vehicles per day, and subject to frequent congestion. The nearest road is at a distance of approximately 35 metres. This site is a part of Automatic Urban and Rural Network (AURN) and is classified as an urban background site.

London Marylebone Road

This site is located on the kerbside of a major arterial route within the City of Westminster in London. The surrounding area forms a street canyon. Traffic flows of over 70,000 vehicles per day pass the site on 6 lanes with frequent congestion. The site is approximately 2 km from the London Bloomsbury site. This site is part of the AURN and is operated by King's College, London, and is classified as a roadside site.

2.2 Description of the Instruments used in the Field Comparison

2.2.1 SMPS and nano-SMPS

The SMPS system comprises a Model 3071A Electrostatic Classifier (EC) which separates the particles into known size fractions, and a model 3022A Condensation Particle Counter (CPC) which measures their concentration. The sample inlet is taken from the output flow of a 16.7 l min^{-1} cyclone having a 50% cut-point at 1.0 μm in order to avoid blockages. Particles larger than the measurement range are removed by inertial impaction. A bipolar charger in the EC is used to charge the particles in the incoming polydisperse aerosol to a known charge distribution, which are then classified according to their electrical mobility. The EC was configured to allow particles in the range 11-450 nm diameter to be counted.

In the CPC the monodisperse aerosol passes through a chamber which is saturated with n-butyl alcohol vapour and then to a cooled condenser where the alcohol condenses onto the particles. Particles are counted as a result of light scattered onto a photodetector after being enlarged to a diameter of about 10 μm.

For more technical details on this instrument, see Wang and Flagan (1990).

The nano SMPS system comprises the Model 3080N nanoclassifier and a Model 3025 Ultrafine Condensation Particle Counter (UCPC). This allows the measurement of particles in the range 5-184 nm and hence will allow the examination of particles in the 5-11 nm range.

2.2.2 *Epiphaniometer*

The epiphaniometer measures the active aerosol surface area that is also called the Fuchs surface of aerosol particles. The measurements depends on the attachment rate of neutral ^{211}Pb atoms onto the surface area of the aerosols (Pandis et al., 1991). The ^{211}Pb atoms are produced at a constant rate by the decay of a short lived radon isotope (^{219}Rn) emanating from a long-lived artificial actinium source (^{227}Ac) that is placed in the attachment chamber of the epiphaniometer. The ^{211}Pb atoms attached to aerosol particles are transported through a capillary to a filter. The attachment coefficient of the ^{211}Pb atoms can be described by the Fuchs theory (e.g. in Seinfeld and Pandis, 1998). The attachment rate is determined by α-spectroscopy via the decay of attached ^{211}Pb atoms (half-life of 36.1 min, needing data inversion see Pandis et al., 1991). The activity is proportional to the total number of atoms attached to the particle surface. The epiphaniometer was calibrated by Matter Engineering (Switzerland) using NaCl monodisperse aerosols of 38 nm, 91 nm and 137 nm.. For more technical details on this instrument, see Gäggeler et al. (1989).

2.2.3 *TEOM, PM_{10} and $PM_{2.5}$ data*

Two Tapered Element Oscillating Microbalances (TEOM) are used to monitor PM_{10} and $PM_{2.5}$ particle mass concentrations at each site. The two TEOMs are identical instruments (Model 1400AB) except for the design of the sampling heads. The particle mass is determined by continuous weighing of particles deposited onto a filter. The filter is attached to a vibrating hollow tapered glass tube whose frequency changes as the mass loading on the filter increases. The vibration frequency is converted to mass concentrations by a microprocessor. Air at 16.67 L min^{-1} is sampled through the PM_{10} impactor inlet and divided between the filter flow (3 L min^{-1}) and an auxiliary flow (13.67 L min^{-1}). For $PM_{2.5}$ measurements, the TEOM is fitted with a Sharp-cut cyclone inlet. The inlet of the TEOMs is heated to 50°C prior to particles being deposited onto the filter in order to eliminate the effect of condensation or evaporation of particle water. This heating of the aerosol stream induces losses of semi-volatile species. Differences between TEOMs and filter-based methods depend on the temperature, the relative humidity and on the concentrations of semi-volatile particulate compounds such as ammonium nitrate (Charron et al., 2003). For that reason, ratios of

gravimetric data/TEOM vary from one day to another and hence the use of basic correction factors is not adequate. Results are for particulate matter involatile at 50°C

2.2.4 *Other instruments*

Data from the carbon monoxide and oxides of nitrogen instruments installed at the sites have been used. These instruments form part of the AURN and the data are quality-assured to national network standards and reported to the UK National Air Quality Data Archive.

For comparison between the different instruments, all data were converted into hourly averages.

3. COMPARISON BETWEEN SMPS AND NANO SMPS DATA

3.1 Results for Bloomsbury

Only the data from 23/02/04 to 04/03/04 at 13:00 is presented due to SMPS malfunctions after the 4th March 2004. The increase in concentrations at the lowest size ranges of the nano SMPS is surprising and will be discussed later (Chapter 4).

For the larger particles a good agreement between the SMPS and the nano SMPS is observed (see figures 3.1 to 3.7). The median ratio SMPS to nano-SMPS reaches 0.9 for particle sizes above 40 nm. The agreement between the two instruments for particle sizes above 100 nm is excellent. Despite larger differences for smaller particles, the correlations found between SMPS and nanoSMPS data for particles below 100 nm are excellent (figures 3.5 & 3.6).

There are two main explanations for differences between the SMPS and the nanoSMPS data:

(1) the counting efficiency of the CPC (model 3022A) is lower for a given particle diameter than the counting efficiency of the UCPC (model 3025A). Size-dependent counting efficiencies are not corrected for.

(2) The SMPS systems do not correct for particle losses in the electrostatic classifier or any other part of the system. The nanoclassifier (model 3080N) has lower losses than the model 3071A classifier.

According to the manufacturer, the Condensation Particle Counter Model 3022A (the one of the SMPS, see figure 3.7a from http://www.tsi.com/particle/downloads/brochures/3022A.pdf) has a counting efficiency of 100% for particles above 50 nm. Its efficiency is above 90% for particles above 30 nm. For particles ranging from 11 to 30 nm, the counting efficiency of the 3022A CPC ranges between 70% for smaller particles and 90% for larger particles.

On the contrary, the counting efficiency of the 3025A UCPC (the one of the nanoSMPS, figure 3.7b from http://www.tsi.com/particle/downloads/brochures/3025A.pdf) is above 95% for particles above 5 nm and virtually 100% for particles above 7 nm.

Birmili (1999) has determined the size-dependent counting efficiency of the 3025 UCPC. Much lower counting efficiency than the ones displayed by TSI are found for particle

diameters below 10 nm. According to Birmili (1999), the counting efficiency reaches 100% at diameters of 30 nm and it is around 90% at diameters of 10 nm.

The ratios of SMPS to nano-SMPS are lower than the counting efficiencies displayed by TSI. Differences between these ratios and counting efficiencies are larger for lower diameters. This suggests that additional losses due to Brownian diffusion or diffusional broadening of very small particles are larger in the SMPS classifier than in the nano classifier.

Birmili et al. (1997) show significant losses of particles below 20 nm in classifiers. They have established an empirical classifier transfer function to correct data.

Excellent correlations are found between the SMPS and nano-SMPS (Figure 3.5) despite divergences at smaller diameters. This means that this comparison could lead to an easy "correction" of SMPS particle numbers for sizes smaller than 40 nm.

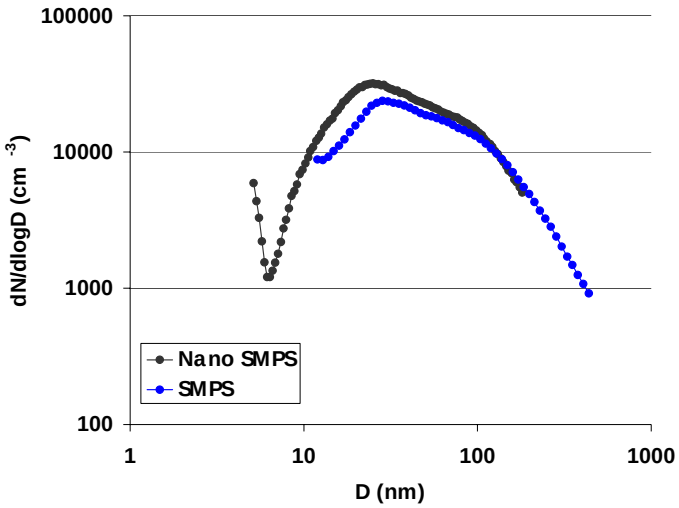

Figure 3.1 : Median particle number size distributions from SMPS and nano SMPS at Bloomsbury (23/02/04 to the 04/03/04)

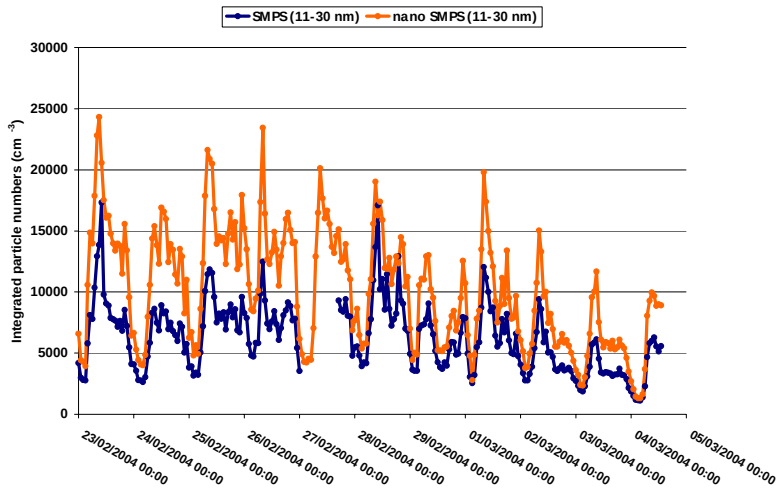

Figure 3.2 : Integrated particle numbers for particle size ranges of 11-30 nm measured with the SMPS (dark blue) and the nano SMPS (orange).
From 23/02/04 to 04/03/04

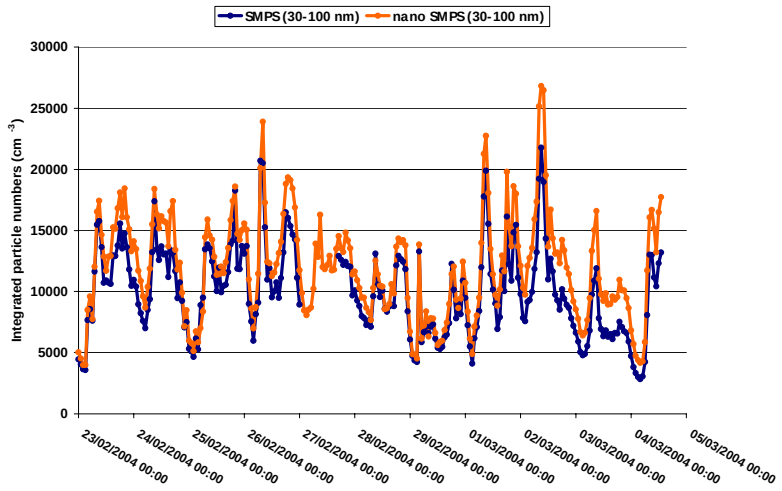

Figure 3.3: Integrated particle numbers for particle size ranges of 30-100 nm measured with the SMPS(dark blue) and the nano SMPS (orange).
From 23/02/04 to 04/03/04

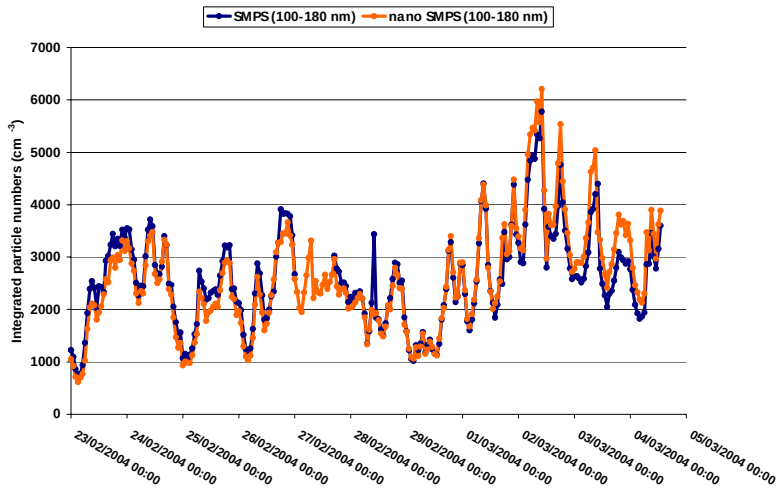

Figure 3.4: Integrated particle numbers for particle size ranges of 100-180 nm measured with the SMPS (dark blue) and the nano SMPS (orange). From 23/02/04 to 04/03/04

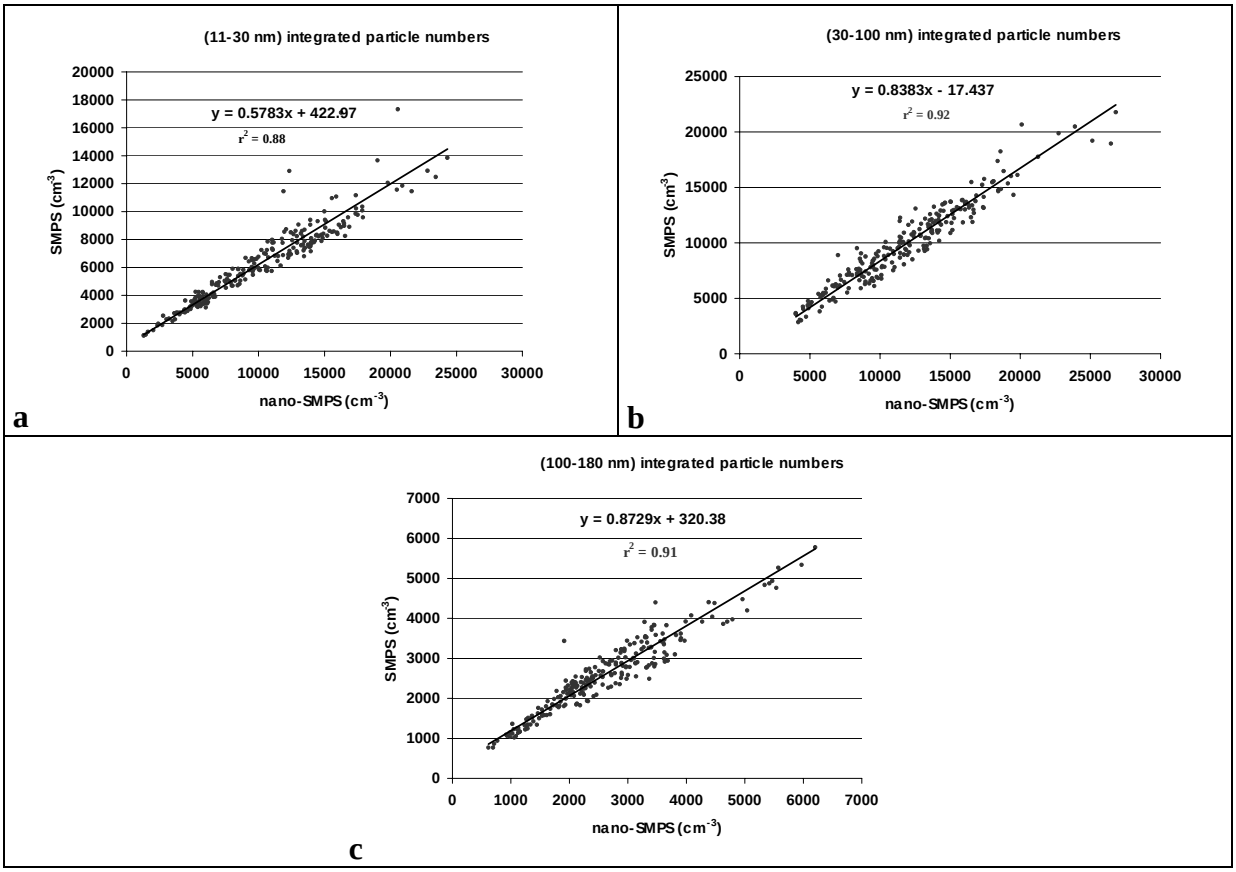

Figure 3.5 : SMPS vs. nano SMPS for (a) 11-30 nm; (b)30-100 nm and (c) 100-180 nm integrated counts. Major axis orthogonal regressions and Pearson correlation coefficients.

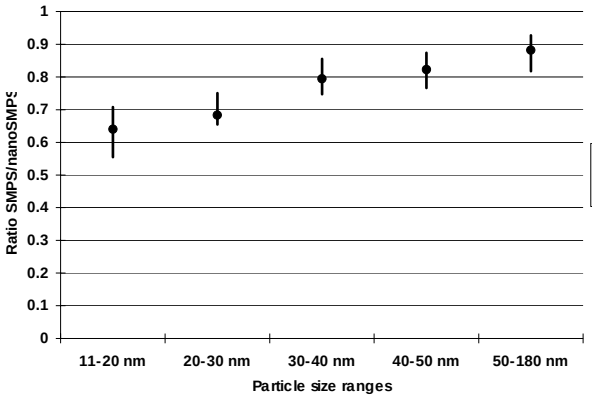

Figure 3.6: Ratio of SMPS to nano-SMPS for different particle size diameters

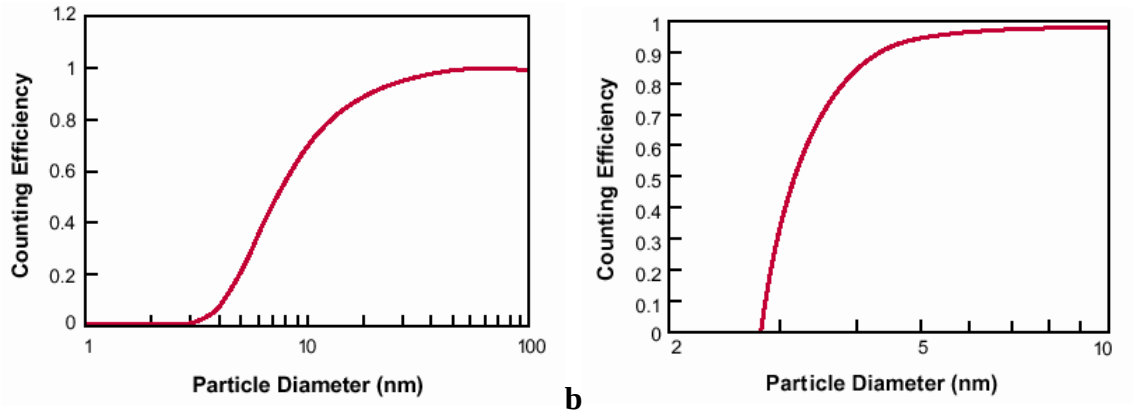

Figure 3.7: (a) Particle-detection efficiency of the 3022A CPC for silver particles in nitrogen at 1500 cm^3/min, normalized data ; (b) Particle-detection efficiency of the 3025A UCPC for NaCl particles in nitrogen at at 1500 cm^3/min, inlet flow. TSI data available on http://www.tsi.com

3.2 Results for Marylebone Road

The dataset is larger than the Bloomsbury one (from 02/10/03 to 18/11/03). There is only a gap in SMPS data from the 26/10/03 to 31/10/03 due to instrument malfunctions.

SMPS data are about 10 times lower than nano SMPS data (see Figures 3.9 to 3.13; note different axes for SMPS and nano SMPS data). Despite this tenfold factor, the correlations are again excellent (even though a bit scattered for particles below 30 nm). There is the same tenfold factor between older SMPS data (e.g. presented in Charron and Harrison, 2003) and data from October to November 2003. This "drop" concerned all the period from May 2003 to July 2004 and it is still unexplained at the time of the writing of this report.

Figure 3.8 shows the excellent agreement between both instruments when SMPS data are multiplied by 10 (except for smaller particle ranges).

Despite this tenfold factor, results again indicate larger differences at smaller diameters than at larger diameters and the same explanations as for the Bloomsbury data could be used.

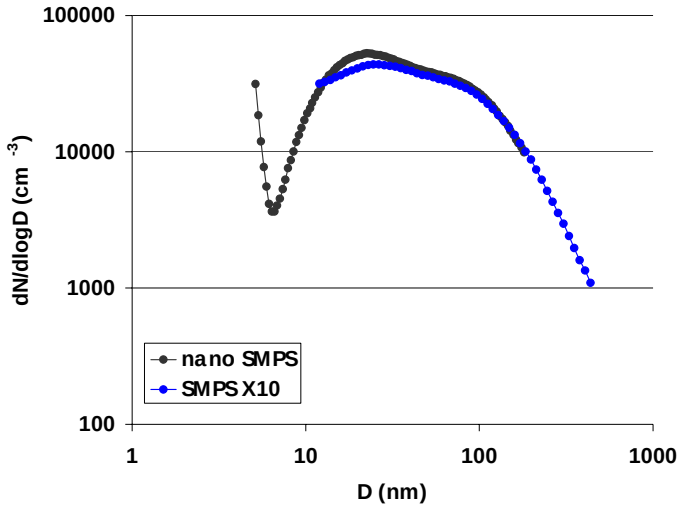

Figure 3.8 : Median particle number size distributions from SMPS (multiplied by 10) and nano SMPS (from 02/10/03 to 18/11/03).

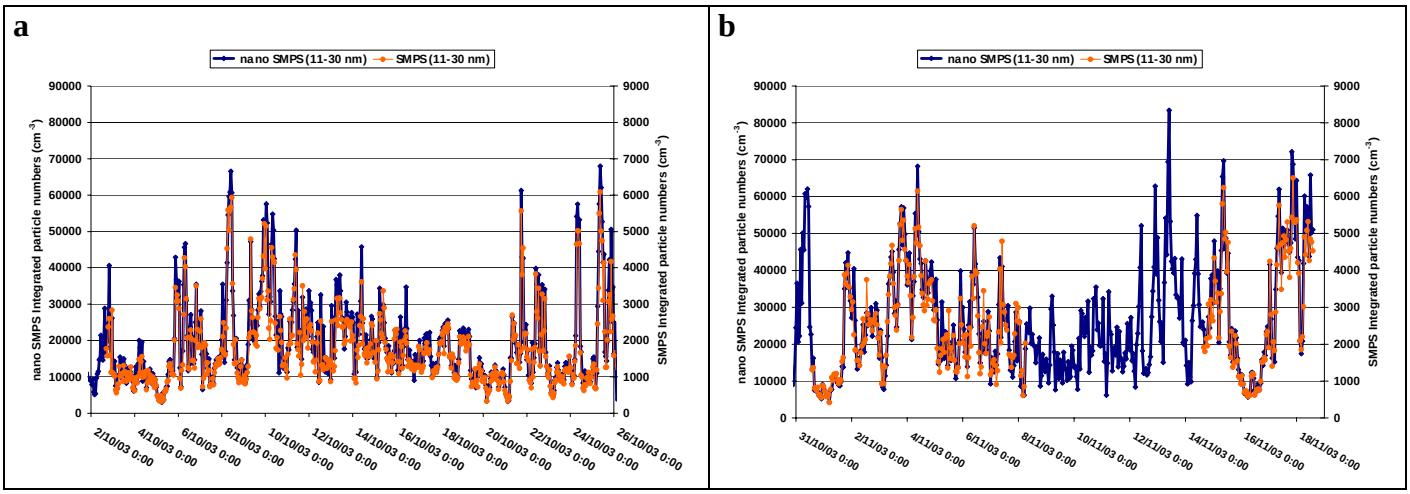

Figure 3.9 : Integrated particle numbers for particle size ranges of 11-30 nm measured with the SMPS (orange) and the nano SMPS (dark blue); (a): from 02/10/03 to 26/10/03 ; (b) : from 31/10/03 to 18/11/03.

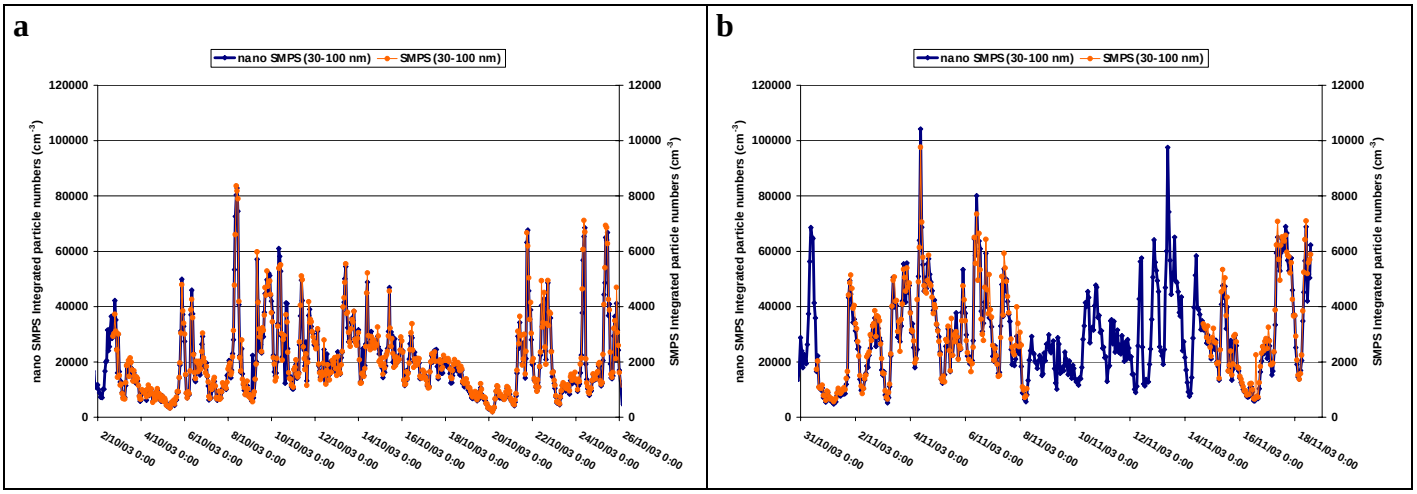

Figure 3.10: Integrated particle numbers for particle size ranges of 30-100 nm measured with the SMPS (orange) and the nano SMPS (dark blue); (a): from 02/10/03 to 26/10/03 ; (b) : from 31/10/03 to 18/11/03.

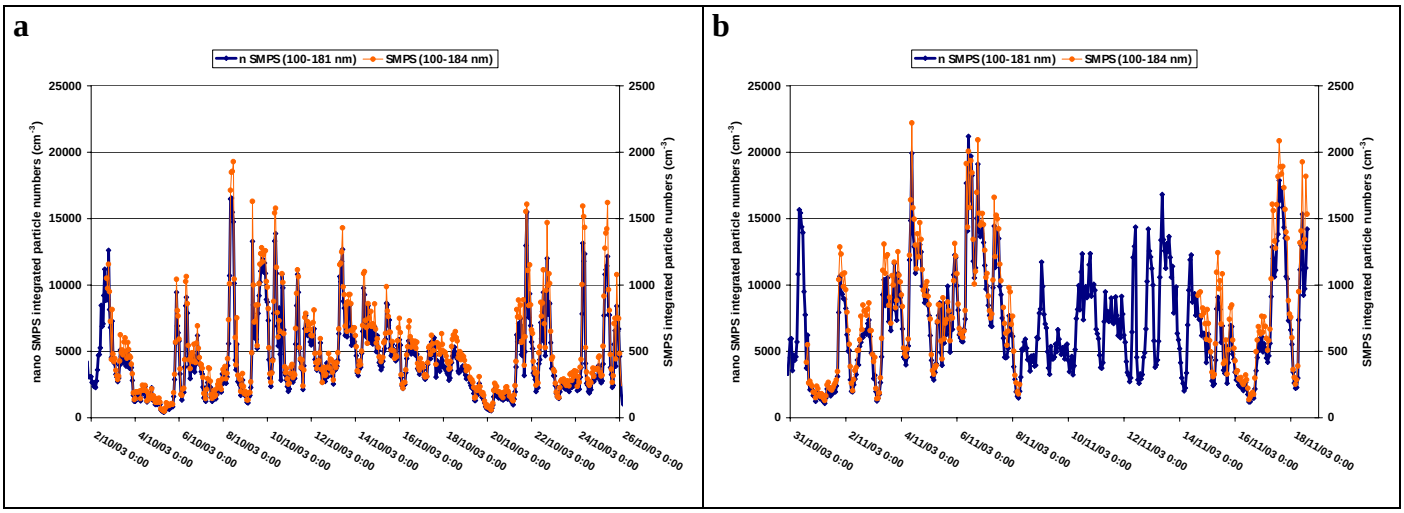

Figure 3.11: Integrated particle numbers for particle size ranges 100-180 nm measured with the SMPS (orange) and the nano SMPS (dark blue); (a): from 02/10/03 to 26/10/03 ; (b) : from 31/10/03 to 18/11/03.

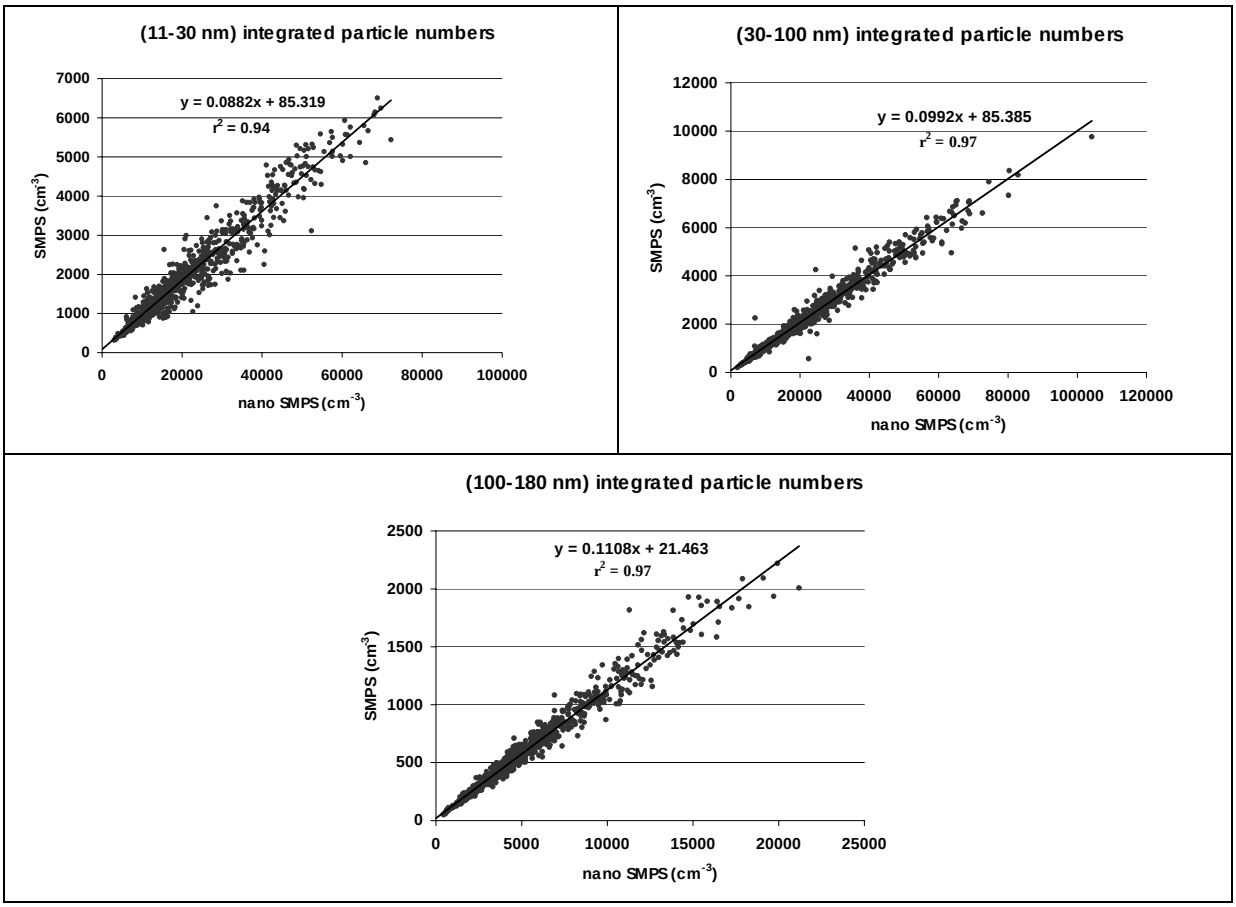

Figure 3.12 : SMPS vs. nano SMPS for (a) 11-30nm ; (b) 30-100 nm; (c) 100-180 nm integrated counts. Major Axis orthogonal regression and Pearson correlation coefficient.

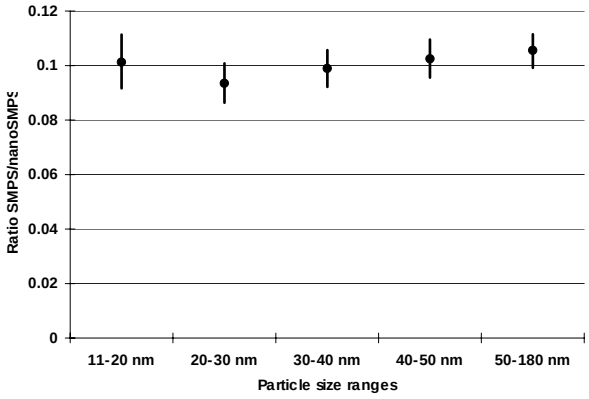

Figure 3.13: Ratio of SMPS to nano-SMPS for different particle size diameters

3.3 Conclusions

An excellent agreement is found between the nano SMPS and the SMPS at Bloomsbury for particle numbers above 100 nm. The SMPS measures lower particle numbers than the nanoSMPS at its lowest size diameters; but excellent linear relationships are found between

both datasets. Both lower counting efficiency by the 3022A CPC at smaller diameters and larger losses by Brownian diffusion of diffusional broadening of small particles by the 3071A classifier could explain lower values by the SMPS since both are not corrected by the SMPS software. The lower concentrations given by the SMPS could satisfyingly be corrected using the comparisons with the nanoSMPS since excellent correlations are found between these two instruments for smaller particles.

Despite a tenfold factor between SMPS and nanoSMPS data at Marylebone Road, excellent correlations for linear relationships are found between both datasets. That suggests that the agreement between the two instruments might be similar to that at Bloomsbury (higher divergences at smaller diameters). The current intercomparison represents the opportunity to correct Marylebone Rd data from May 2003 to July 2004 (the drop of SMPS data by a factor 10 concerns all this period).

4. ASSESSMENT OF PARTICLES BELOW 11 NM (MINIMUM SIZE TO BE COUNTED AT BLOOMSBURY AND MARYLEBONE ROAD)

The current configuration of the Scanning Mobility Particle Sizers installed at Marylebone Road and Bloomsbury limits the minimum size of particles counted to 11 nm in diameter. The nano SMPS was installed at Bloomsbury and Marylebone Road during short periods in order to measure particles down to 5 nm. Due to instrument malfunctions, only particles down to 7 nm are studied in this report.

Particle number size distributions measured at Bloomsbury and Marylebone Road (Figure 4.1) show a mode at sizes between 20 and 30 nm, a shoulder between 50 and 90 nm (suggesting the existence another mode merged with the large one) and suggests another mode which peaks below 5 nm.

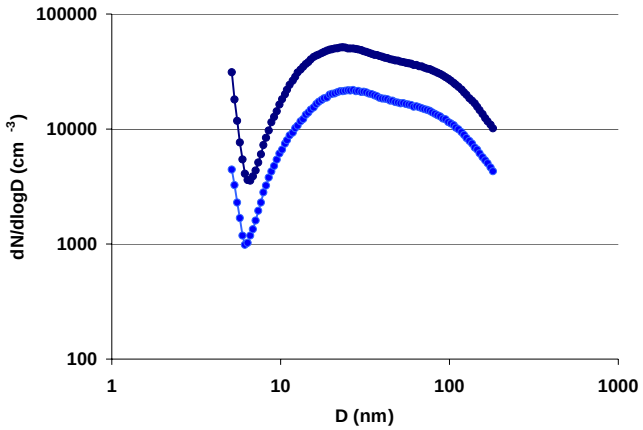

Figure 4.1: Median particle number size distributions at Marylebone Road (dark blue) and Bloomsbury (light blue)

Average particle number size distributions in Figure 4.1 reach a minimum around 7 nm and particle numbers increase for diameters below 7 nm. This pattern is common at Bloomsbury and Marylebone Road and is always observed at the two sites (morning, afternoon, night). Concentrations of sub 7 nm particles are much higher at Marylebone Road than at Bloosmbury. Such a pattern is rarely observed anywhere else where particle number size distributions are generally “closed” to the left in absence of new particle formation (e.g. Woo et al., 2001 ; Wehner et al., 2002). It is therefore most probable that these sub 7 nm particles are an artefact.

Table 4.1 presents the 25, 50 (median) and 75 percentiles of the concentrations measured during these periods and the percentage of particles ranging from 7 to 11 nm respectively for Bloomsbury and Marylebone Road data. Numbers of particles ranging from 7 to 11 nm represent on average 5% (median) of particle numbers covering the entire range of the nanoSMPS at both sites (see also figures 4.1 & 4.2). Similar proportions are found at Bloomsbury and Marylebone Road.

		% $N_{(7-11)}$	$N_{(7-11)}$	$N_{(11-30)}$	$N_{(30-100)}$	$N_{(100-450)}$
Bloomsbury	**P0.25**	4.3	668	4563	5959	1288
	P0.50	5.5	1035	7229	8933	2008
	P0.75	6.7	1489	10573	12269	2737
Marylebone Rd		% $N_{(7-11)}$	$N_{(7-11)}$	$N_{(11-30)}$	$N_{(30-100)}$	$N_{(100-450)}$
	P0.25	4.1	1501	11836	12491	2828
	P0.50	5.2	2447	18317	20317	4713
	P0.75	6.8	4362	30112	32493	7923

Table 4.1: 25, 50 and 75 Percentiles of integrated particle numbers for particle size ranges of 7-11 nm, 11-30 nm, 30-100 nm and 100-180 nm measured with the nano SMPS and percentages of particle numbers below 11 nm for Bloomsbury and Marylebone Road (in comparison the entire range measured by the nano SMPS i.e. 5-180 nm)

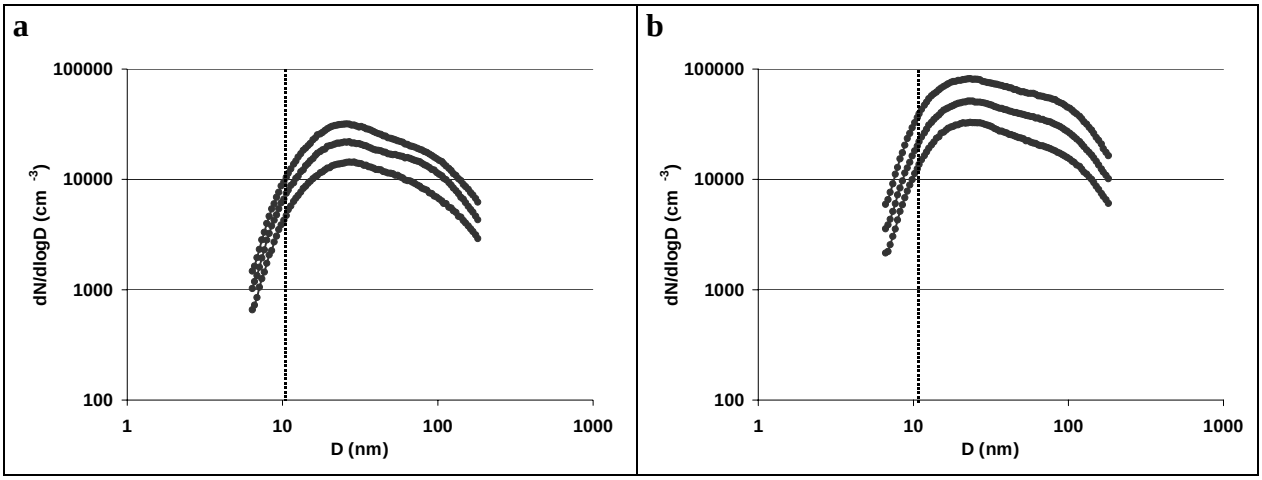

Figure 4.2: 25, 50 and 75 Percentiles of particle number size distributions for (a) Bloomsbury (from the 23/02/04 to the 27/03/04) and (b) Marylebone road (from 25/09/03 to 19/11/03)

5. COMPARISON BETWEEN THE ACTIVE AEROSOL SURFACE AREA DERIVED FROM THE EPIPHANIOMETER AND SURFACES CALCULATED FROM SMPS MEASUREMENTS

Work under the previous contract (Shi et al., 2001) has shown a good agreement between the active surface from an epiphaniometer and the one calculated from the size distribution determined by a combination SMPS/Aerodynamic particle sizer (APS).

In this report, epiphaniometer data are compared with surfaces derived from SMPS data (this chapter) and with other particle metrics and gases (next chapter) in order to assess whether the active particle surface area could be derived from current measurements for use in epidemiological studies.

5.1 Active Surface Area of Particles from the Epiphaniometer

The epiphaniometer is described in detail by Gäggeler et al. (1989). Short-lived gaseous ^{211}Pb atoms are delivered by a ^{227}Ac source. The ^{211}Pb atoms attach onto aerosol particles which are collected on a filter. The activity is then measured by an alpha detector. Calibration experiments (Gäggeler et al., 1989 ; Rogak et al., 1991) have shown that the attachment coefficient of the lead atoms can be described by the Fuchs coagulation theory and the measured signal is proportional to the "Fuchs surface" of the aerosol particles.

According to the Fuchs theory, at small aerodynamic diameters (below 100 nm, free molecular regime) the epiphaniometer signal is proportional to the square particle diameter, d^2. At large aerodynamic diameters (above 3 µm, hydrodynamic regime), the signal is proportional to the particle diameter, d. In the intermediate regime, the signal is proportional to d^x, with x is a function of the particle diameter, $x \in [1,2]$. For a polydisperse aerosol the obtained signal is the integral of the differential products dN.dS with N the particle concentration and S the "active aerosol surface".

The active aersol surface area is an important particle metric. It represents the area accessible for interactions between the aerosol particles and atoms or molecules of the surrounding gas. As a consequence, the active aerosol surface area has a significance in many aerosol processes such as heterogeneous chemistry or interactions with biological systems.

5.2 Calculation of the Active Surface Area

5.2.1 *Surface area assuming that particles are spherical*

The “geometric” surface is computed from SMPS data assuming that particles are spherical:

$$S_G = \pi d^2$$

S_G is the surface of particles of d diameter. The total “geometric” surface is:

$$TotalGeometricSurface = \sum S_G(d) \cdot N(d)$$

This surface is called “geometric surface” or S_G in the report.

5.2.2 *Surface area calculated from the Fuchs coagulation coefficient K_{12}*

$$S_F = \pi d^x$$

with x varying between 1 and 2 as a function of the particle diameter:

$$x(d) = \frac{\ln K_{12}(d) - \ln K_{12}(d_0)}{\ln(d) - \ln(d_0)}$$

d_0 is 1 µm by definition, K_{12} is the coagulation coefficient between 1 and 2 (in this case, coagulation between the aerosol particles and the lead atoms). For definition of K_{12}, see e.g. Seinfeld and Pandis (1998). x(d) has been calculated by Pandis et al. (1991) for a hydrated lead atom estimated of 1.5 nm diameter (figure 5.1).

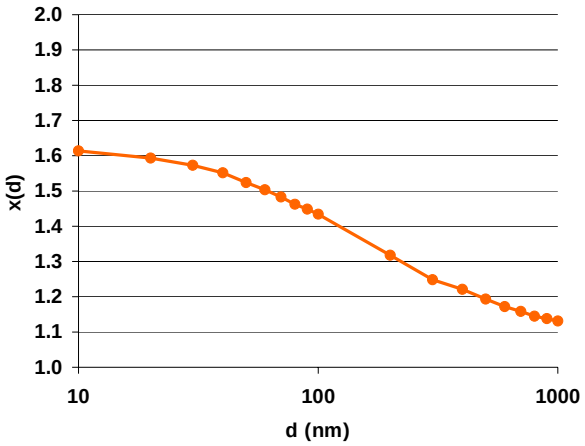

Figure 5.1: Exponent x [equations (1) and (2)] as a function of the aerosol diameter for a lead cluster diameter of 1.5 nm. From Pandis et al., 1991

The total surface area of a polydisperse aerosol will be the integral of the different products:

$$TotalFuchsSurface = \sum S_F(d) \cdot N(d)$$

This surface is called "Fuchs surface" or S_F in the report.

5.2.3 *Surface area calculated from the mobility of particles*

For small particles, the active surface area is inversely proportional to the mobility of the particles.

$$S_{active} = \frac{\varphi \cdot \lambda}{1.5 \cdot \eta} \cdot \frac{1}{b}$$

η is the viscosity of air, $\eta = 1.81.10^{-5}$ Ns/m^2

λ is the mean free path of gas molecules in the air, λ=66 nm

φ is a scattering parameter, φ = 1.695

with b, the particle mobility is a function of the particle diameter:

$$b(D_p) = \frac{C_c(D_p)}{3\pi\eta \cdot D_p}$$

D_p is the particle diameter

$$C_c(D_p) = 1 + \frac{2\lambda}{D_p}\left(A + Q \cdot e^{-\beta \cdot \frac{D_p}{2\lambda}}\right)$$ is the Cunningham correction factor

A, Q, β are the Cunningham parameters,

$$A_{Hinds} = 1.17;\ Q_{Hinds} = 0.525;\ \beta_{Hinds} = 0.78$$

Then, the surface active will be:

$$S_{active} = \pi D_p^2 \frac{2\lambda \cdot (A+Q)}{D_p + 2\lambda \cdot \left(A + Q e^{-\beta \cdot \frac{D_p}{2\lambda}} \right)}$$

This surface is called “active surface” or S_A in the report.

5.3 Results for Bloomsbury

The surface area measured by the epiphaniometer using the factory calibration is appreciably different than the ones computed from SMPS data (either “geometric”, “Fuchs” or “Active” surfaces), see figures 5.3 to 5.8. This result was expected for the geometric surface, but it was not expected for the Fuchs and the active surfaces. Additionally, the surface area computed from SMPS data was expected to be smaller than the one derived from epiphaniometer measurements, which is not the case (SMPS measurements cover a smaller range of particle diameters than the epiphaniometer). Also very surprising, the Fuchs surface and the active surface area computed from SMPS data gives different estimates of the surface. Nevertheless, an “exceptional” linear relationship is found between these two estimates (see Figure 5.9a). Excellent linear relationships are also found between the geometric surface and the active surface (Figure 5.9b) and between the geometric surface and the Fuchs surface (Figure 5.9c). Contrary to us, Shi et al. (2001) have found a good agreement between epiphaniometer data and Fuchs surfaces from the SMPS/APS combination (the contribution of the APS was small at the urban background site).

On the other hand, good power-fit relationships with correlation coefficients above 0.8 are found between surfaces computed from SMPS data and the epiphaniometer surface (Figures 5.4; 5.6; 5.8). Best fitting by power relationships indicates larger divergences between epiphaniometer surface and surfaces computed from SMPS measurements at higher surface concentrations. Surprisingly, relationships are not improved by computing the Fuchs and the active surfaces than computing the geometric surface.

Bloomsbury epiphaniometer surface measurements were 10 times lower than epiphaniometer surface measurements during the Birmingham campaign (in Shi et al., 2001) and also lower than epiphaniometer measurements during the Harwell campaign (in Shi et al., 2001).

All these results suggest a calibration problem, probably arising at the factory.

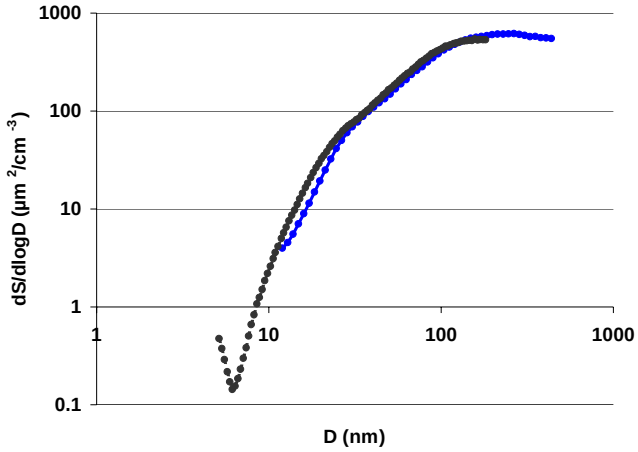

Figure 5.2: Median particle surface size distributions at Bloomsbury
from SMPS measurements (in blue) and nano SMPS measurements (in black)

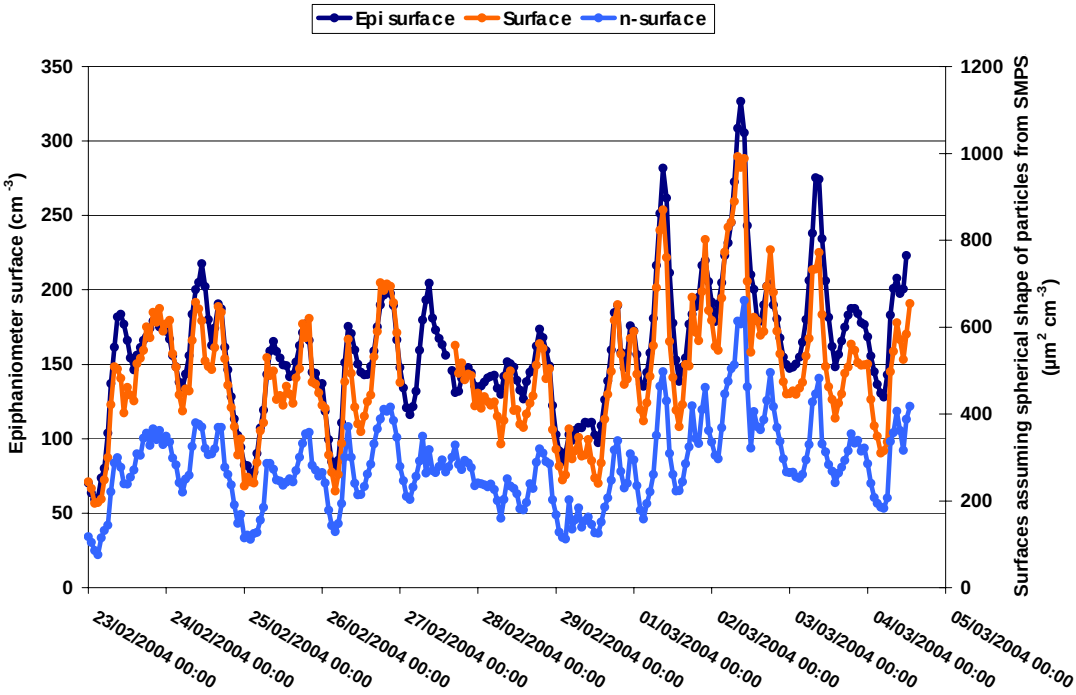

Figure 5.3: Epiphaniometer surface (dark blue) and surfaces assuming spherical shape of particles computed from SMPS data (orange) and nano SMPS data (light blue), Bloomsbury

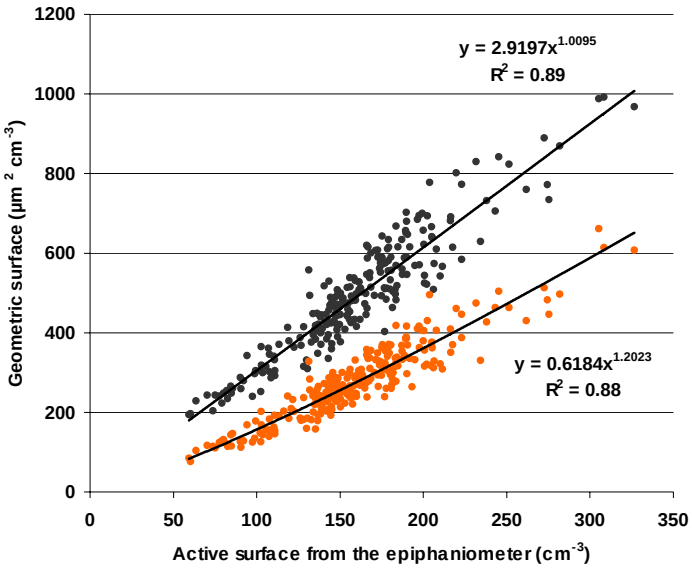

Figure 5.4 : Bloomsbury, surface assuming spherical shape of particles from SMPS vs. epiphaniometer surface (black) and surface assuming spherical shape of particles from nanoSMPS vs. epiphaniometer surface (orange)

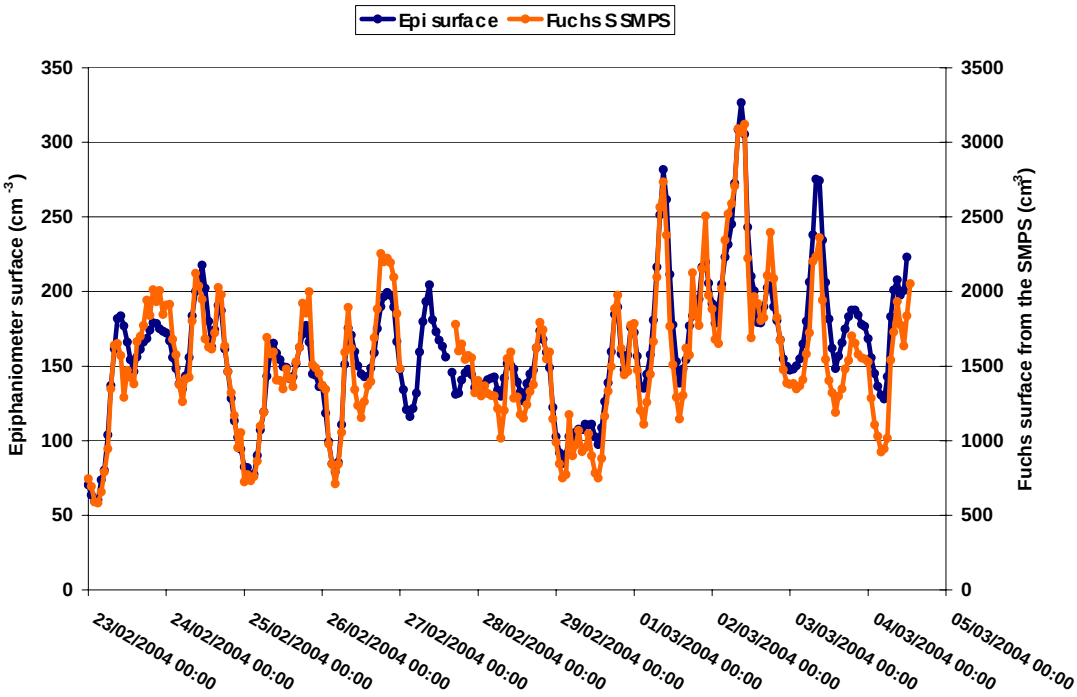

Figure 5.5: Epiphaniometer surface (dark blue) and Fuchs surface computed from SMPS data (orange), Bloomsbury

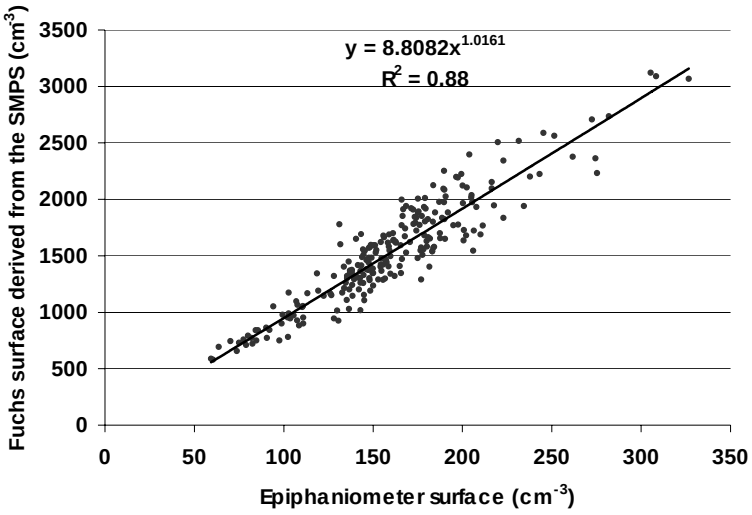

Figure 5.6 : Bloomsbury, Fuchs surface from SMPS vs. Epiphaniometer surface

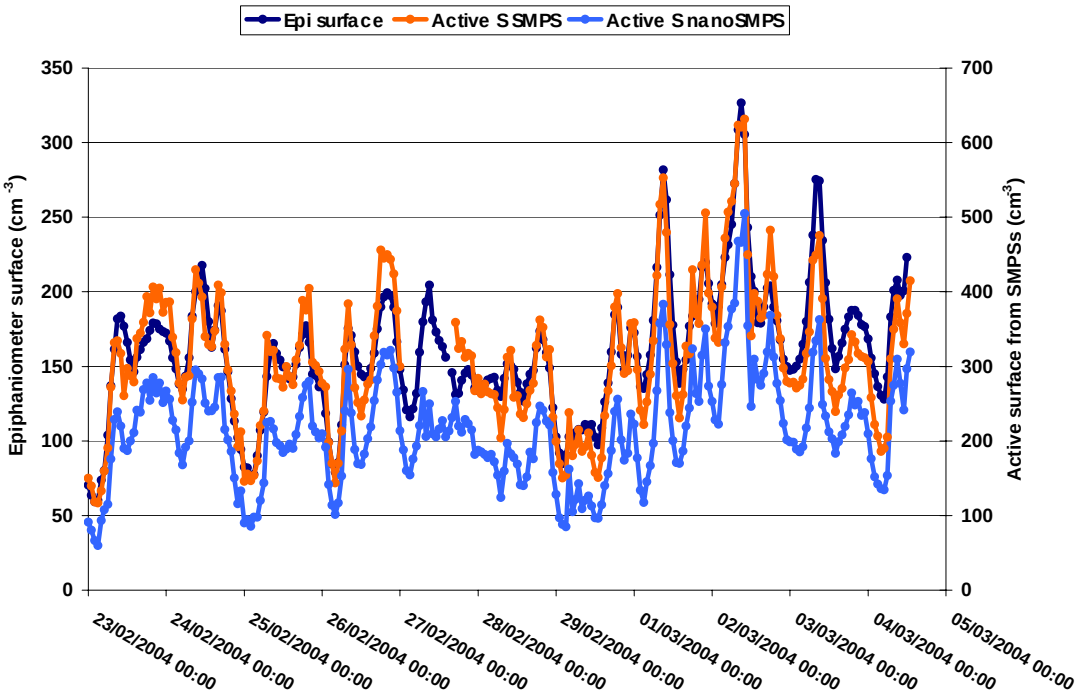

Figure 5.7: Epiphaniometer surface (dark blue) and active surfaces computed from SMPS data (orange) and nano SMPS data (light blue), Bloomsbury

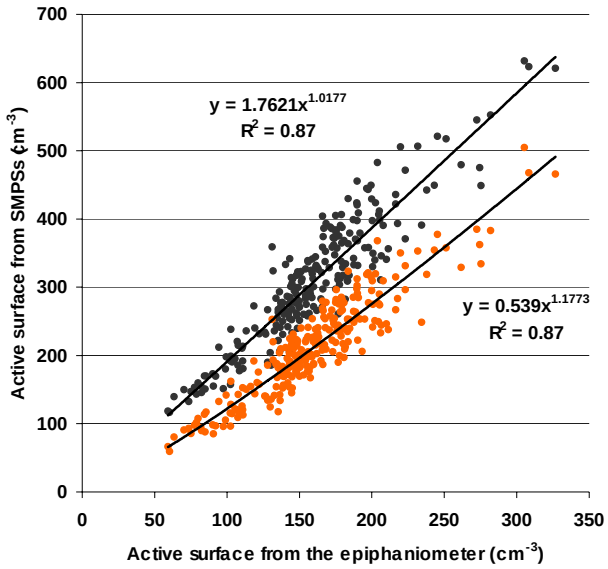

Figure 5.8 : Bloomsbury, Active surface from SMPS vs. Epiphaniometer surface (black) and active surface from nanoSMPS vs. Epiphaniometer surface (orange)

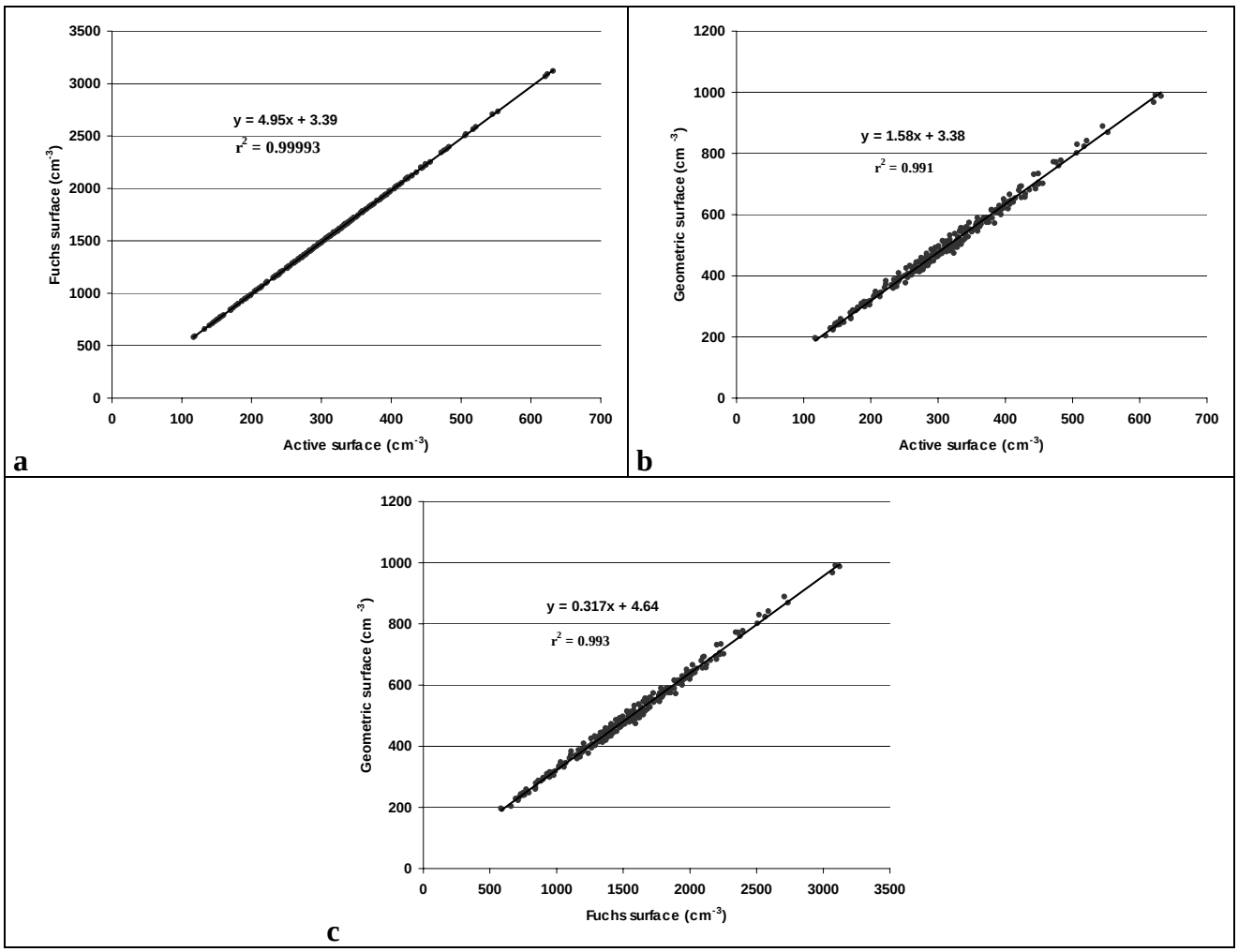

Figure 5.9: Bloomsbury, relationships between different surfaces computed from SMPS measurements (a) Fuchs surface vs. Active surface ; (b) Geometric surface vs. Active surface ; (c)) Geometric surface vs. Fuchs surface (all fitted models are major-axis orthogonal regression)

5.4 Results for Marylebone Road

Similarly to Bloomsbury data, the surface area measured by the epiphaniometer and those computed from SMPS measurements are different (even when SMPS are multiplied by 10; see Figures 5.11 to 5.16). Again, the relationships between the surface derived from the epiphaniometer and surfaces calculated from SMPS data are well-fitted by power-relationships. Now, the powers are around 1.2 (they were very close to 1 at Bloomsbury) (see Figures 5.10, 5.12, 5.14). However, the relationships again have correlation coefficients above 0.8 (Figures 5.11; 5.13; 5.15). Actually, divergences between surfaces from SMPS measurements and epiphaniometer data are larger at higher surfaces and those divergences are larger than those at Bloomsbury.

As with Bloomsbury data, the active surface and the Fuchs surface are different and an exceptional relationship is found between these two estimates. Relationships found between the active surface, the Fuchs surface and the geometric surface are similar to the ones found with Bloomsbury data (except for the intercepts). Now the intercepts are not significantly different than 0 and the following factors could be derived from these relationships (Figure 5.17):

- Factor 4.94 between S_F and S_A,
- Factor 1.53 between S_G and S_A,
- Factor 0.31 between S_G and S_F.

Except in Figure 5.10 (comparison between particle surface size distributions from nano SMPS and SMPS), the SMPS data are not multiplied by 10 for comparisons with epiphaniometer data.

Again, epiphaniometer data measured at Marylebone Road are much lower than those measured during the Birmingham intercomparison of the previous contract (Shi et al., 2001).

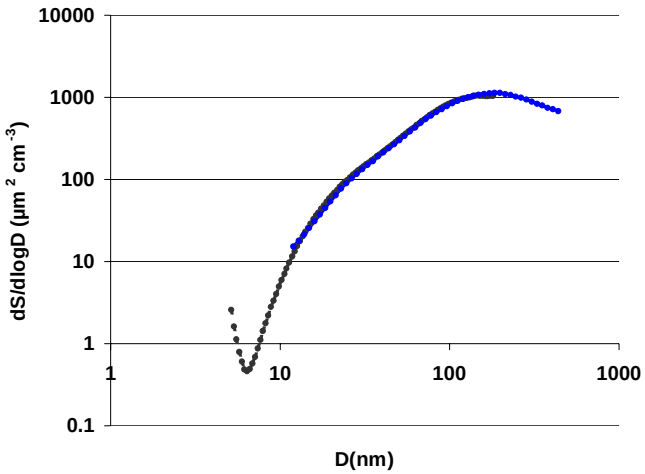

Figure 5.10: Median particle surface size distributions at Marylebone Road from SMPS measurements multiplied by 10 (in blue) and nano SMPS measurements (in black)

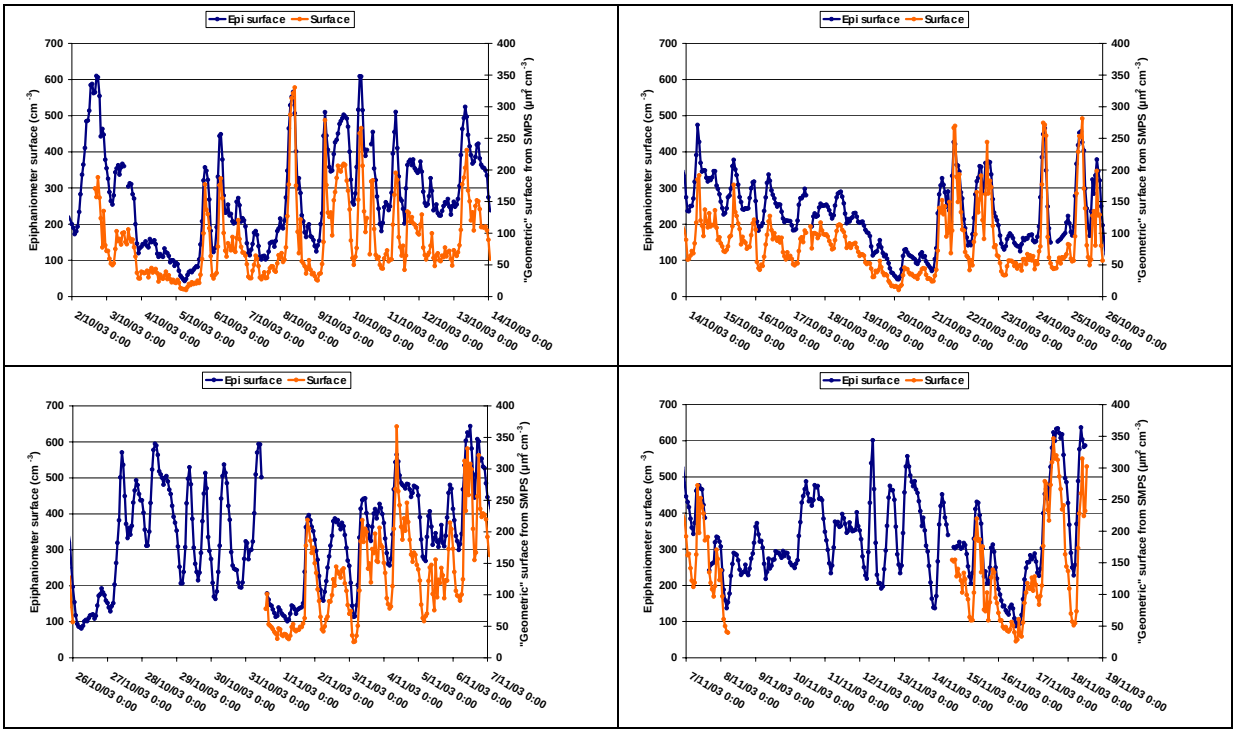

Figure 5.11: Aerosol active surface from the epiphaniometer (dark blue) and surfaces assuming spherical shape of particles from SMPS data (orange), Marylebone Road

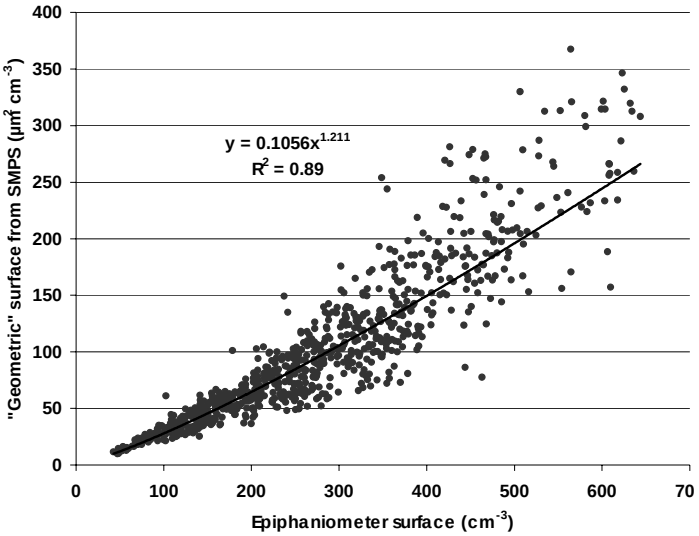

Figure 5.12 : Marylebone Road, surface from SMPS assuming spherical shape of particles vs. Epiphaniometer surface

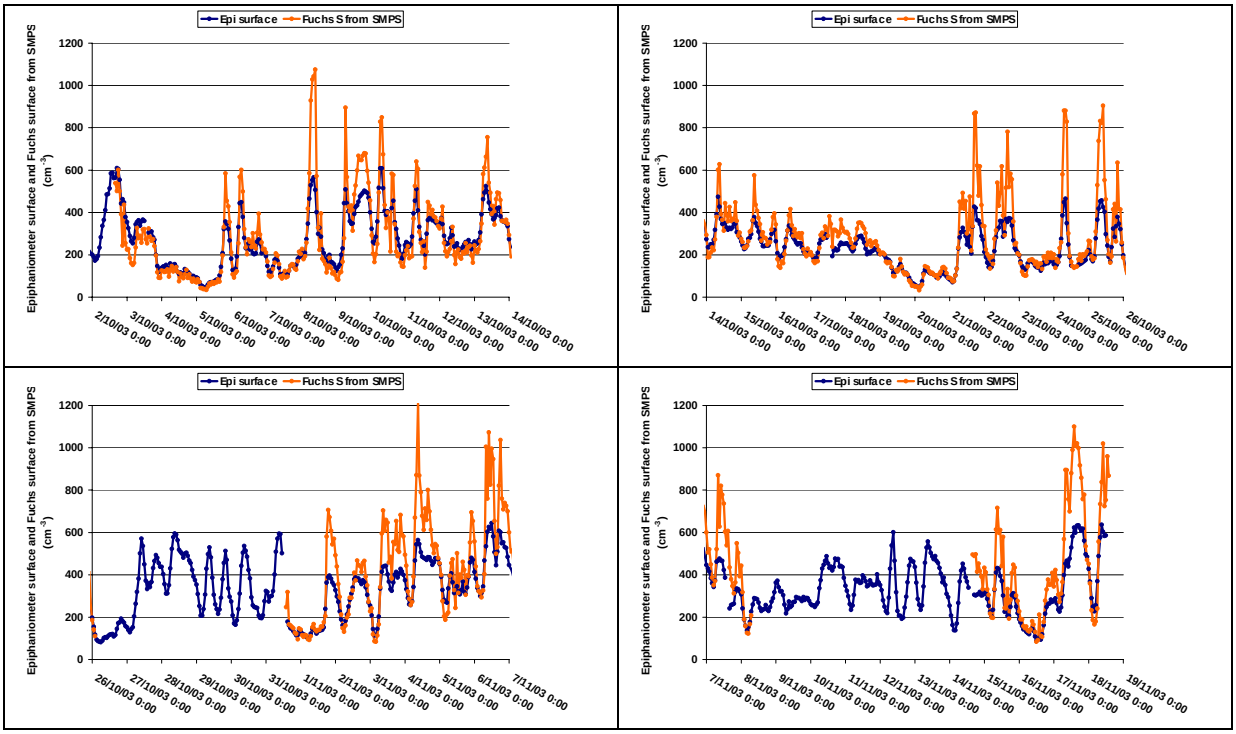

Figure 5.13: Epiphaniometer surface (dark blue) and Fuchs surface computed from SMPS data (orange), Marylebone Road

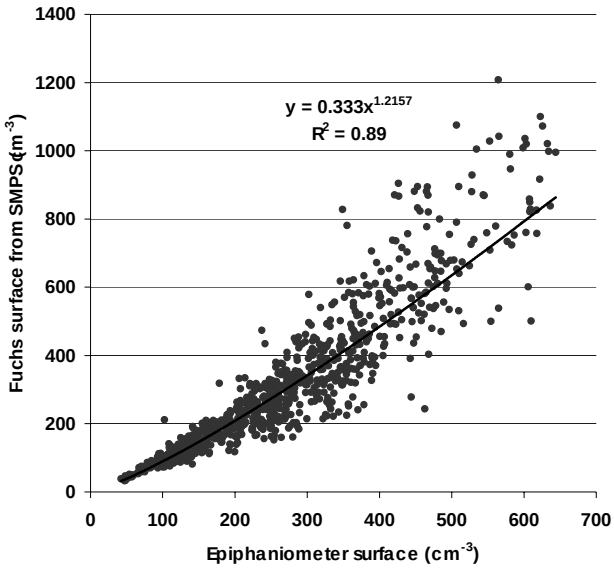

Figure 5.14 : Marylebone Road, Fuchs surface from SMPS vs. Epiphaniometer surface

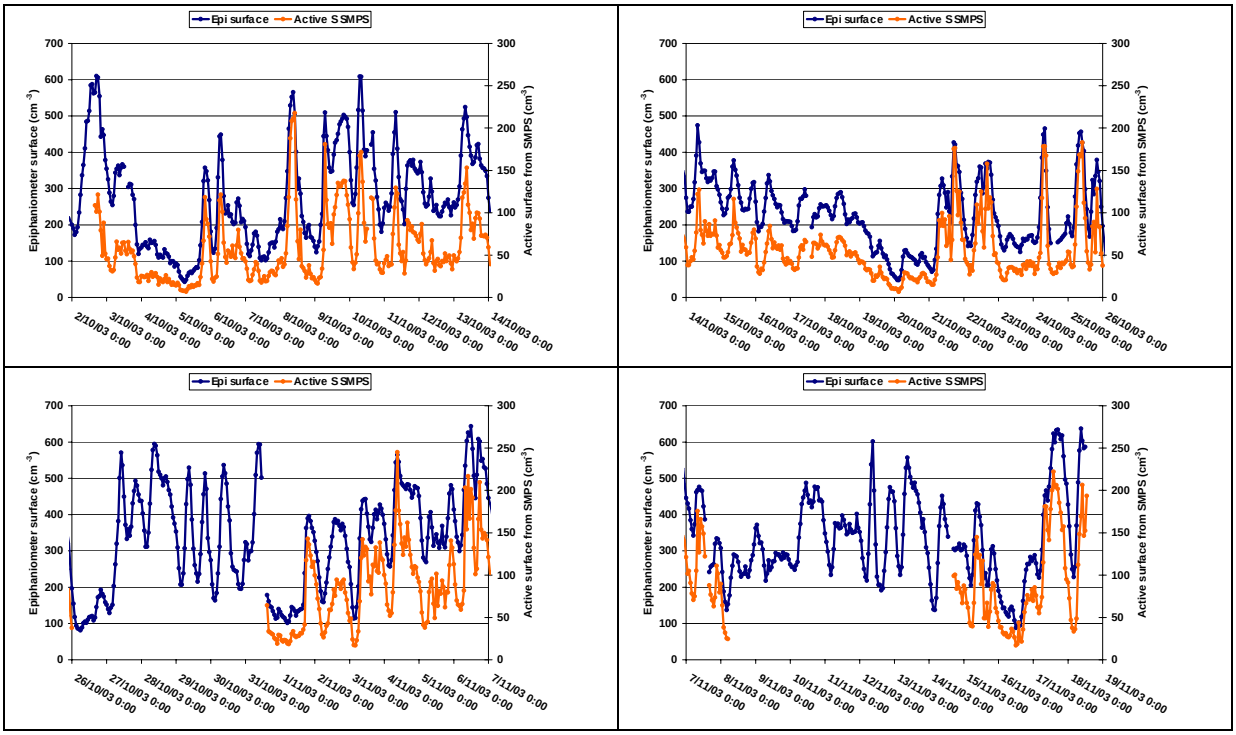

Figure 5.15: Aerosol active surface from the epiphaniometer (dark blue) and active surfaces computed from SMPS data (orange), Marylebone Road

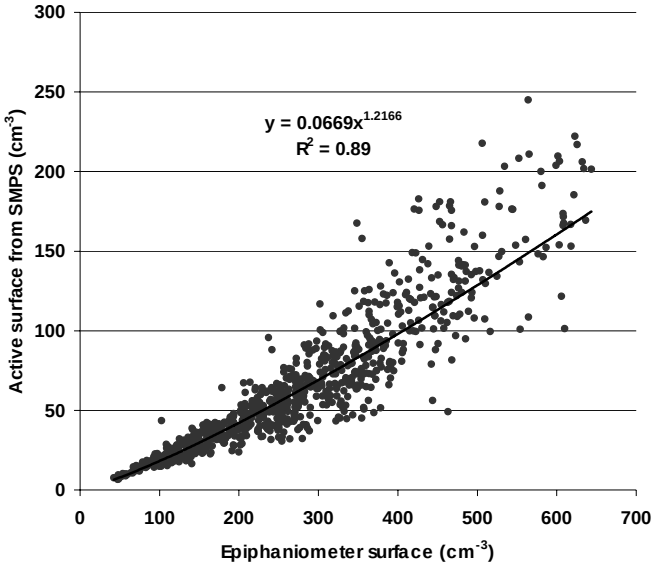

Figure 5.16 : Marylebone Road, Active surface from SMPS vs. Epiphaniometer surface

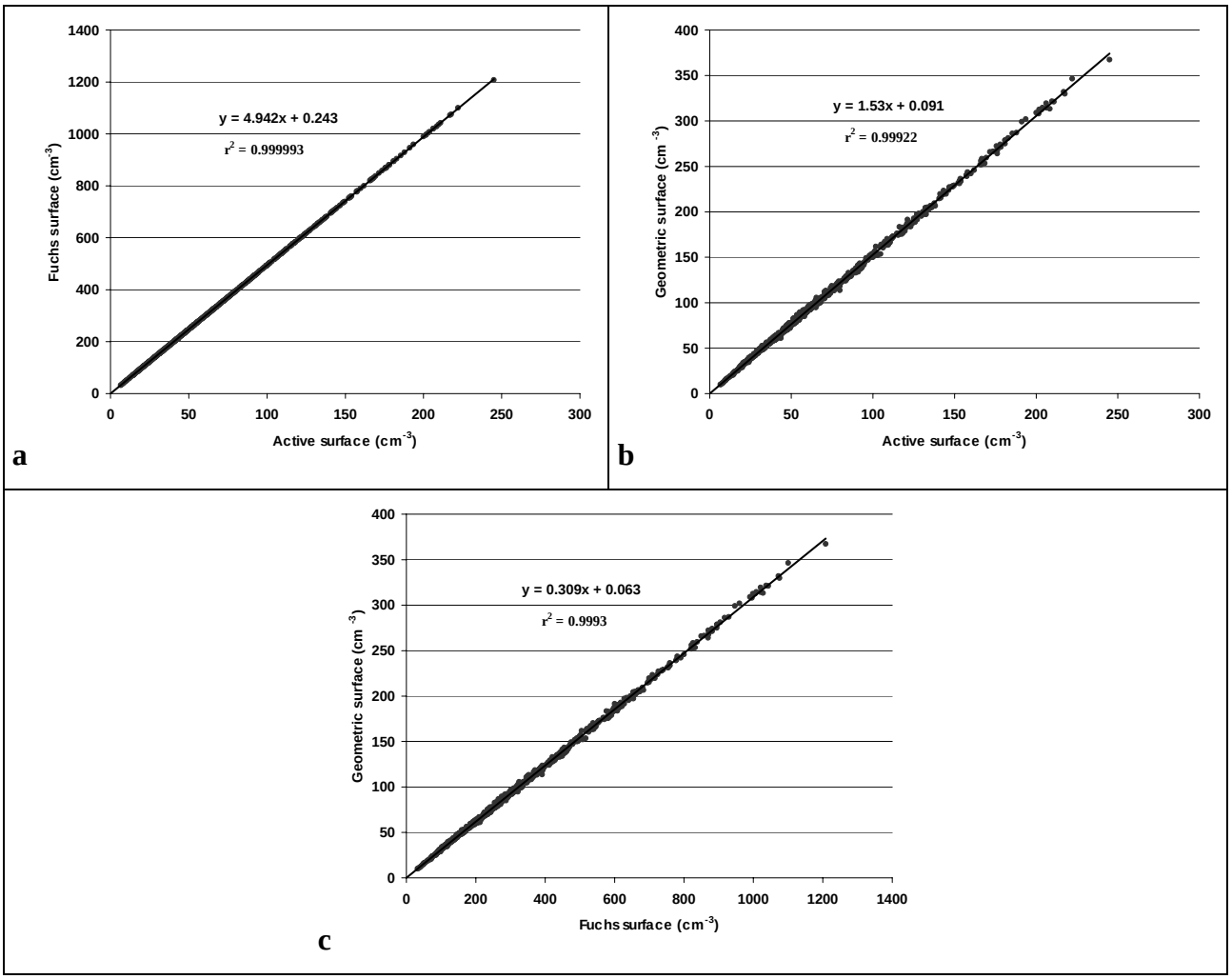

Figure 5.17: Maylebone Road, relationships between different surfaces computed from SMPS measurements (a) Fuchs surface vs. Active surface; (b) Geometric surface vs. Active surface; (c) Geometric surface vs. Fuchs surface (all fitted models are major-axis orthogonal regression)

5.5 Conclusions

Contrary to our expectations, it was not possible to assess the surface measured by the epiphaniometer using SMPS measurements.

Formulae established from the Fuchs coagulation coefficient and the one established from particle mobility give estimates of the surface with a factor of approximately 5 of difference. Also, the computed surface assuming that particles are spherical (πd^2) seems to be related to the active surface and to the Fuchs surface by constant factors.

Power relationships fit the relationships between surfaces computed from SMPS measurements and epiphaniometer surfaces ($r^2>0.80$). The calculation of the Fuchs surface or active surface from SMPS data does not give better relationships than the calculation of the geometric surface (πd^2).

The reasons for these discrepancies are unknown at the time of the writing of the report. A calibration problem and an unsuitable equation might explain these results.

6. RELATIONSHIPS BETWEEN THE THREE PARTICLE METRICS (NUMBER, SURFACE, MASS) AND GAS PHASE MEASURES OF TRAFFIC POLLUTION

In order to examine (1) whether particle numbers or particle surface area could be derived from more widely measured particle metrics or gases such as NO_x or CO and/or (2) to inform future air monitoring strategies, relationships between particle numbers, mass and surface and between these three particle metrics and CO/NO_x are examined in this chapter using hourly and daily concentrations.

Results presented in this chapter are provisional since discrepancies have been shown between instruments (Chapter 5).

6.1 Relationships with Hourly Data

Spearman correlation coefficients between hourly concentrations (Table 6.1) show significant correlations at the 1% level between all paired data for both sites. Those significant correlations are likely the result of common sources and common dispersion processes that influence the concentrations of the different particle metrics and gases. However, better correlations are found at Marylebone Road where the local traffic emissions strongly dominate measured concentrations. At Bloomsbury, particle concentrations arise from the mixing of different urban emissions, including traffic.

The best relationships with the epiphaniometer surface are found with particle numbers above 100 nm. This is in agreement with that particle surface size distributions peak above 100 nm (Figures 5.2 & 5.9, chapter 5) and that the fine fraction (0.1 to 1 µm) of the aerosol makes the greatest contribution to the surface area. Nevertheless, no strong relationship is found between the epiphaniometer surface and the fine particle mass ($PM_{2.5}$). Correlations between epiphaniometer data and SMPS data are better when surfaces (whatever the surface) are calculated (chapter 5). Therefore, only relationships between total integrated particle numbers from SMPS data will be discussed in this chapter.

Despite these significant correlations, Figure 6.1 shows that the relationships are very scattered; especially those with epiphaniometer data. This result shows that hourly epiphaniometer data could not be satisfactorily derived from current measures at urban sites. Figure 6.2 shows that Marylebone Road relationships are much better but still very scattered.

	Fuchs surface from the epiphaniometer		Total particle number from the SMPS		Total particle number from the nano SMPS	
Spearman's rho	Bloomsbury	Marylebone Rd	Bloomsbury	Marylebone Rd	Bloomsbury	Marylebone Rd
Fuchs surface	1	1	0.50 237	0.92 826	0.82 759	0.91 1273
S_Total N	0.50 237	0.92 826	1	1	0.98 238	0.98 838
S_11-30 nm		0.81 826	0.85 238	0.95 842	0.84 238	0.95 838
S_30-100 nm	0.54 237	0.92 826	0.97 238	0.98 842	0.95 238	0.96 838
S_100-450 nm	0.91 237	0.94 826	0.51 238	0.95 842	0.49 238	0.92 838
nS_Total N	0.82 759	0.91 1273	0.98 238	0.98 838	1	1
nS_7-11 nm	0.76 759	0.68 1273	0.73 238	0.79 838	0.74 781	0.84 1295
nS_11-30 nm	0.65 759	0.79 1273	0.86 238	0.92 838	0.92 781	0.96 1295
nS_30-100 nm	0.84 759	0.93 1273	0.90 238	0.97 838	0.96 781	0.97 1295
nS_100-180 nm	0.84 759	0.95 1273	0.34 238	0.94 838	0.69 781	0.93 1295
PM_{10}	0.62 746	0.86 1287	0.44 238	0.87 833	0.51 768	0.85 1284
$PM_{2.5}$	0.68 747	0.87 1223	0.24 238	0.84 762	0.49 769	0.81 1217
CO	0.70 747	0.83 1248	0.61 237	0.89 789	0.69 768	0.87 1245
NO_X	0.81 746	0.88 1291	0.81 237	0.96 832	0.86 767	0.95 1288
NO	0.75 539	0.88 1291	0.81 237	0.96 832	0.80 551	0.95 1288
O_3	-0.67 539	-0.58 1242	-0.48 237	-0.62 784	-0.58 551	-0.57 1236

Table 6.1: Spearman correlations coefficients between hourly concentrations of different particle metrics and gas phase measures of traffic pollution measured at Bloomsbury and Marylebone Road. The significance is below 0.001 (2-tailed).

Key: S= SMPS; ns = nano-SMPS

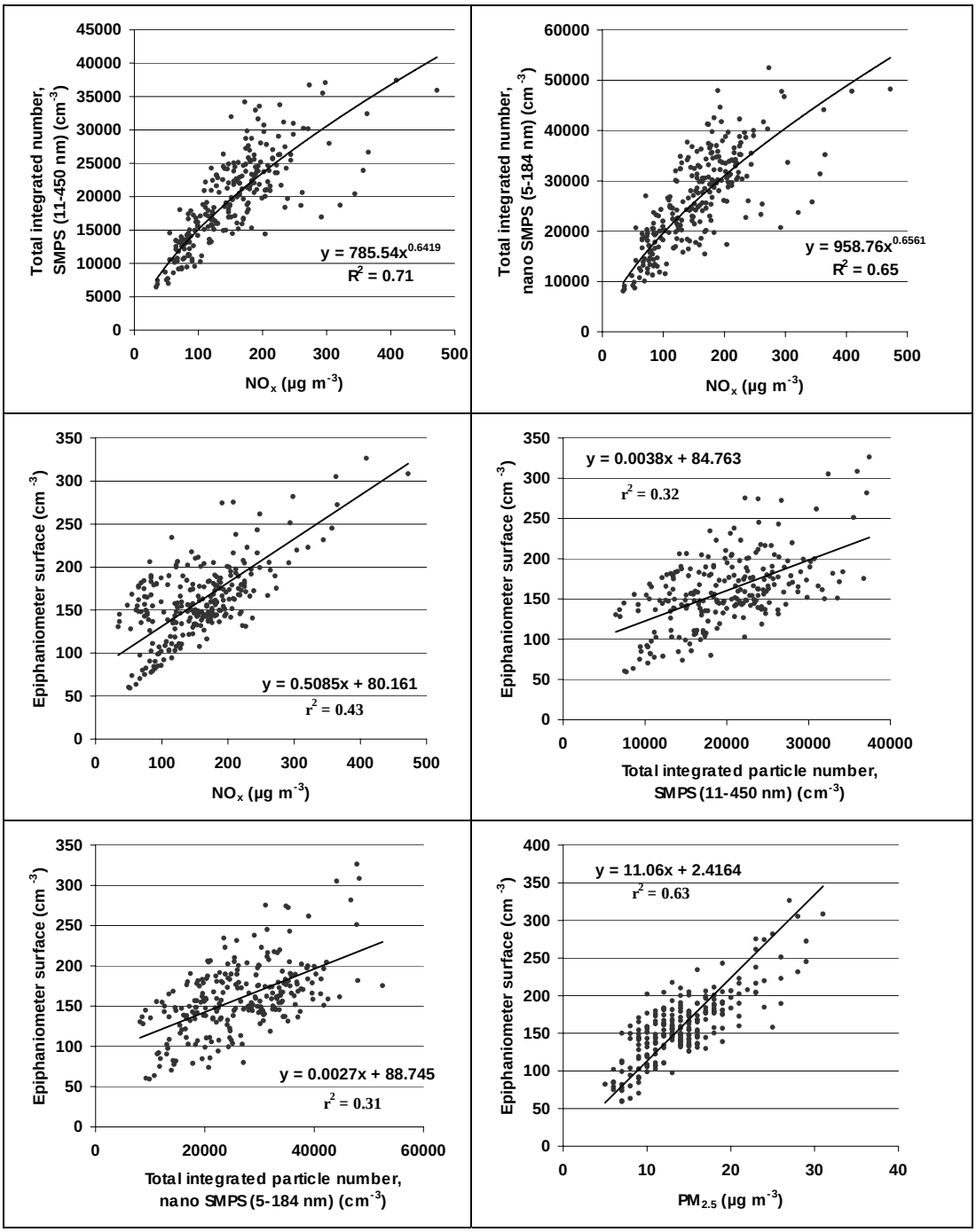

Figure 6.1: Best fit relationships for hourly concentrations of total integrated numbers and epiphaniometer surface, Bloomsbury (now the correlation coefficients are the Pearson ones).

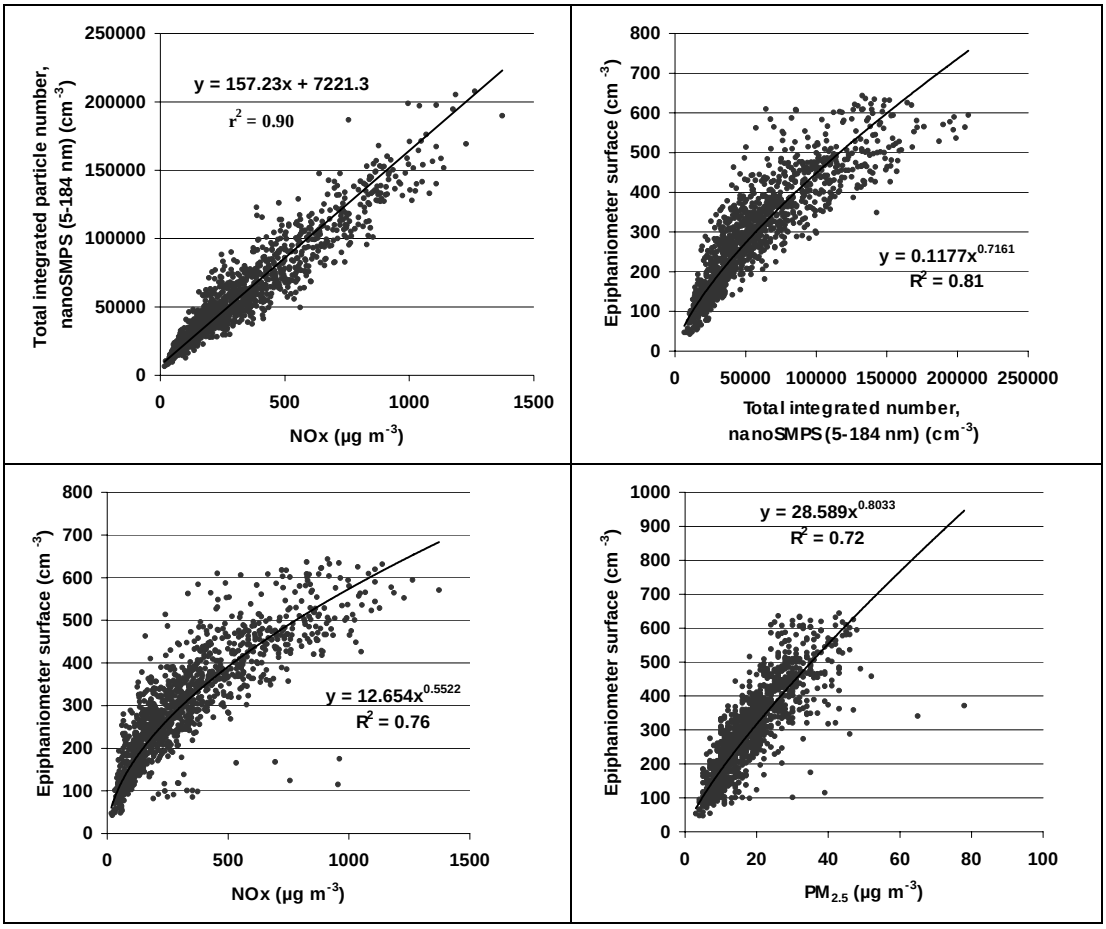

Figure 6.2: Best fit relationships for hourly concentrations of total integrated numbers and epiphaniometer surface, Marylebone Road

6.2 Relationships with Daily Data

Correlations are much better when daily average values are considered. The very small SMPS dataset for Bloomsbury is mainly responsible for many non-significant correlation coefficients (Table 6.2).

Very good relationships are found between the epiphaniometer surface and NO_x concentrations and between total integrated particle numbers and NO_x concentrations for both Bloomsbury and Marylebone Road datasets (Figures 6.3 & 6.4). For Marylebone Road, the relationship between the epiphaniometer data and total integrated particle numbers and the relationships between the epiphaniometer data and PM_{10} concentrations are also very close.

	Fuchs surface from the epiphaniometer		Total particle number from the SMPS		Total particle number from the nano SMPS	
Spearman's rho	Bloomsbury	Marylebone Rd	Bloomsbury	Marylebone Rd	Bloomsbury	Marylebone Rd
Fuchs surface	1	1		0.93 (0.000) 30	0.82 (0.000) 29	0.89 (0.000) 48
S_Total N		0.93 (0.000) 30	1	1	0.78 (0.013) 9	0.99 (0.000) 35
S_11-30 nm		0.87 (0.000) 30	0.75 (0.020) 9	0.97 (0.000) 35		0.97 (0.000) 35
S_30-100 nm		0.94 (0.000) 30	0.73 (0.016) 10	0.99 (0.000) 35	0.68 (0.042) 9	0.98 (0.000) 35
S_100-450 nm	0.98 (0.000) 9	0.93 (0.000) 30		0.96 (0.000) 35		0.94 (0.000) 35
nS_Total N	0.82 (0.000) 29	0.89 (0.000) 48	0.78 (0.013) 9	0.99 (0.000) 35	1	1
nS_7-11 nm	0.43 (0.004) 29	0.75 (0.000) 48	0.70 (0.036) 9	0.90 (0.000) 35	0.71 (0.000) 33	0.93 (0.000) 55
nS_11-30 nm	0.64 (0.000) 29	0.80 (0.000) 48	0.83 (0.005) 9	0.96 (0.000) 35	0.88 (0.000) 33	0.98 (0.000) 55
nS_30-100 nm	0.88 (0.000) 29	0.91 (0.000) 48		0.98 (0.000) 35	0.95 (0.000) 33	0.98 (0.000) 55
nS_100-180 nm	0.78 (0.000) 29	0.96 (0.000) 48		0.94 (0.000) 35	0.62 (0.000) 33	0.92 (0.000) 55
PM_{10}	0.62 (0.000) 28	0.88 (0.000) 46		0.83 (0.000) 34	0.46 (0.010) 31	0.80 (0.000) 52
$PM_{2.5}$	0.61 (0.001) 28	0.86 (0.000) 46		0.87 (0.000) 31	0.37 (0.038) 32	0.72 (0.000) 51
CO	0.77 (0.000) 28	0.83 (0.000) 46		0.93 (0.000) 32	0.72 (0.000) 32	0.92 (0.000) 52
NO_X	0.79 (0.000) 27	0.89 (0.000) 46		0.98 (0.000) 32	0.84 (0.000) 31	0.98 (0.000) 52
O_3	-0.78 (0.000) 21	-0.76 (0.000) 46		-0.76 (0.000) 32	-0.68 (0.000) 23	-0.75 (0.000) 51

Table 6.2: Spearman correlations coefficients between daily concentrations of different particle metrics and gas phase measures of traffic pollution measured at Bloomsbury and Marylebone Road. The p-values are in brackets. The correlation coefficient is not written when the correlation is not significant at the 5% level (p-values > 0.05)

Key: S = SMPS; ns = nano-SMPS

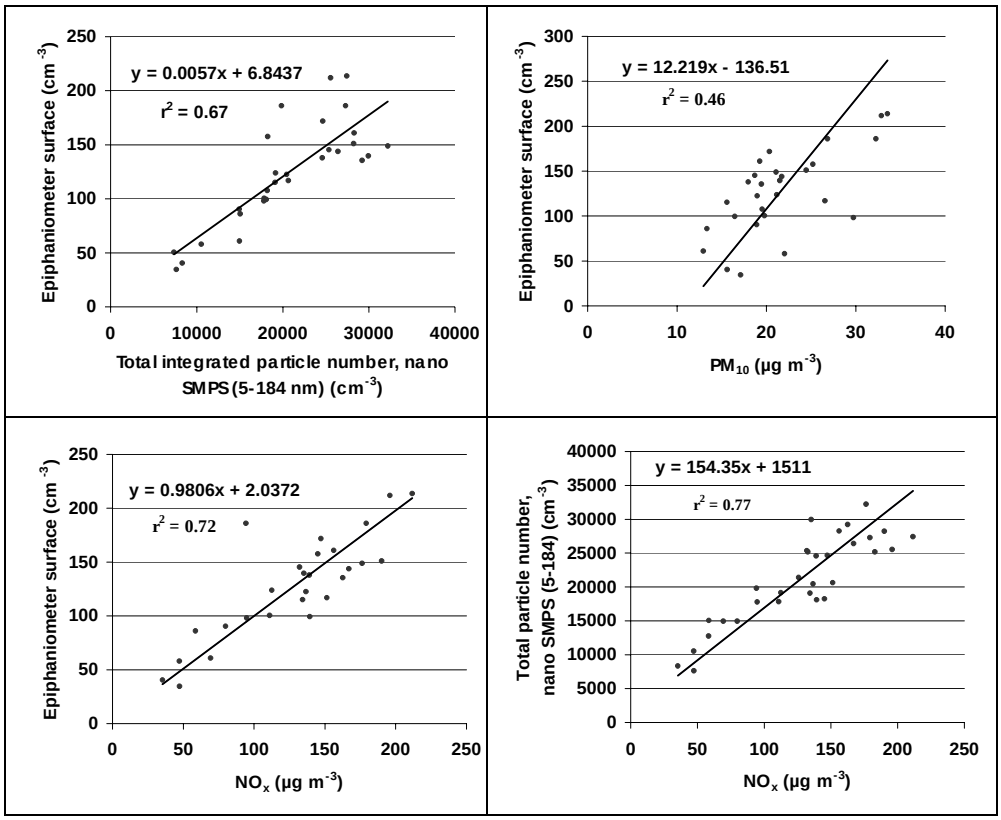

Figure 6.3: Best fit relationships for daily concentrations of total integrated numbers and epiphaniometer surface, Bloomsbury

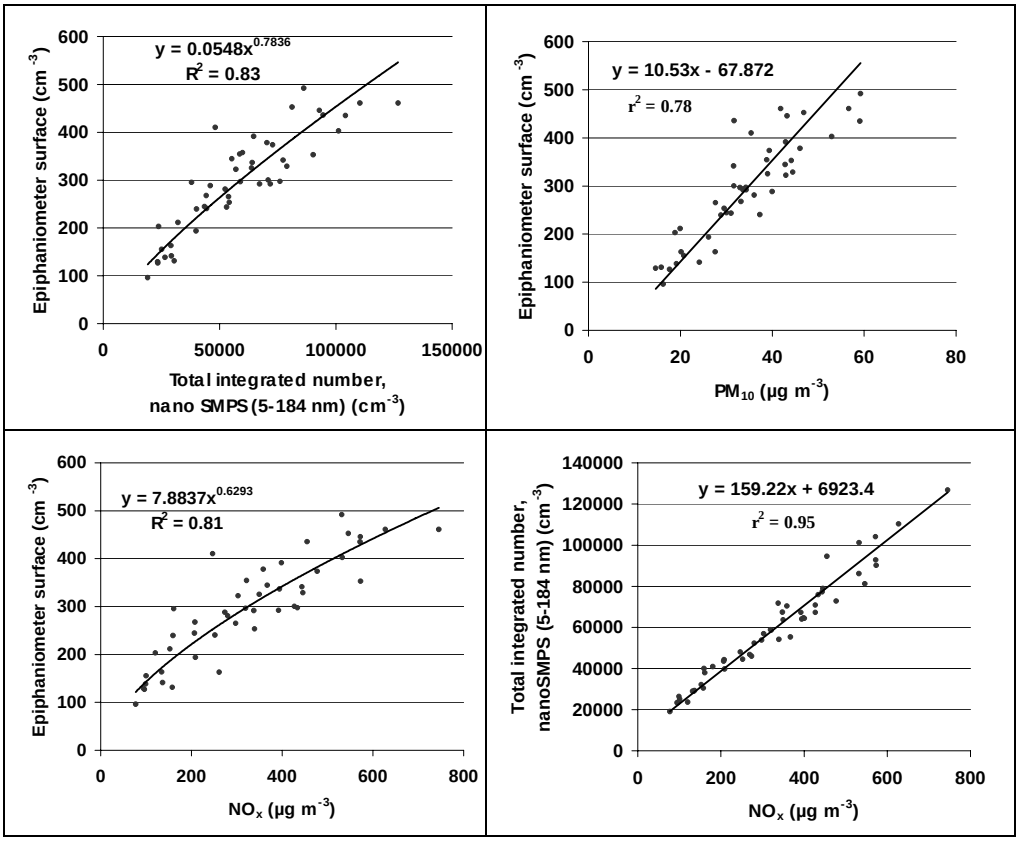

Figure 6.4: Best fit relationships for daily concentrations of total integrated numbers and epiphaniometer surface, Marylebone Road

7. ACKNOWLEDGEMENTS

To Dr. Andrew Allen (University of Birmingham) and Dr. David Harrison (Casella Stanger) for running the instruments and supplying the data.

To Matter Engineering (Switzerland) for supplying on loan the epiphaniometer and calibrations.

To Markus Kasper (Matter Engineering) and Gil Sem (TSI) for discussions.

8. REFERENCES

Birmili, W., 1999, Production of new ultrafine aerosol particles in continental air masses, PhD dissertation, Leipzig University, VWF Verlag für Wissenschaft und Forschung GmbH, Berlin.

Charron, A., and Harrison, R. M., 2003, Primary particle formation from vehicle emissions during exhaust dilution in the roadside atmosphere., Atmospheric Environment, 37, 4109-4119.

Charron, A., Harrison, R. M., Moorcroft, S., Booker, J., 2004, Quantitative interpretation of divergence between PM_{10} and $PM_{2.5}$ mass measurement by TEOM and gravimetric (Partisol) instruments., Atmospheric Environment, 38, 415-423.

Donaldson, K., Li, X. Y., MacNee, W., 1998, Ultrafine (nanometre) particle mediated lung injury, Journal of Aerosol Science 29, pp 553-560.

Gäggeler, H. W., Baltensperger, U., Emmenegger, M., Jost, D. T., Schmidt-Ott, A., Haller, P., Hofmann M., 1989, The epiphaniometer, a new device for continuous aerosol particle monitoring, Journal of Aerosol Science 20, pp 557-564.

Harrison, R. M., Jones, M., Collins, G., 1999, Measurements of the physical properties of particles in the urban atmosphere, Atmospheric Environment 33, pp 309-321.

Keywood, M. D., Ayers, G. P., Gras, J. L., Gillett, R. W., Cohen, D. D., 1999, Relationships between size segregated mass concentration data and ultrafine particle number concentrations in urban areas., Atmospheric Environment 33, pp 2907-2913.

Maynard, A. D., Maynard, R. L., 2002, A derived association between ambient aerosol surface area and excess mortality using historic time series data., Atmospheric Environment, 36, pp 5561-5567.

Molnár, P., Janhall, S., Hallquist, M., 2002. Roadside Measurements of Fine and Ultrafine Particles at a Major Road North of Gothenburg., Atmospheric Environment 36, pp 4115-4123.

Morawska, L., Johnson, G., Ristovski, Z. D., Agranovski, V., 1999, Relation between particle mass and number for submicrometer airborne particles., Atmospheric Environment 33, pp 1983-1990.

Oberdorster, G., 2000. Toxicology of Ultrafine Particles: *In Vivo* Studies. Phil. Trans. R. Society, London. A. 358, 2719-2740.

Pandis, S. N., Baltensperger, U., Wolfenbarger, J. K., Seinfeld, J. H., 1991, Inversion of aerosol data from the epiphaniometer, Atmospheric Environment 22, pp 417-428.

Rogak, S. N., Baltensperger, U., Flagan, R. C.,1991, Measurement of mass transfer to agglomerate aerosols. Aerosol Science and Technology 14, pp 447-458.

Seinfeld, J. H., Pandis, S. N., Atmospheric chemistry and physics from air pollution to climate change., New York, pp. Pages, 1996.

Shi, J. P., Harrison, R.M., Evans, D., 2001, Comparison of ambient particle surface area measurement by epiphaniometer and SMPS/APS, Atmospheric Environment 35, pp 6193-6200.

Tuch, Th., Brand, P., Wichmann, H. E., Heyder, J., 1997, Variation of particle number and mass concentration in various size ranges of ambient aerosols in Eastern Germany, Atmospheric Environment 31, pp4193-4197.

Wang, S.C., and Flagan, R.C., 1990. Scanning Electrical Mobility Spectrometer. Aerosol Science and Technology 13, 230-240

Wehner, B., Birmili, W., Gnauk, T. and Wiedensohler, A., 2002. Particle Number Size Distributions in a Street Canyon and their Transformation into the Urban-Air Background: Measurements and a Simple Model Study. Atmospheric Environment 36, 2215-2223.

Woo, K. Chen, S.D.R., Pui, D.Y.H. and McMurry, P.H., 2001. Measurement of Atlanta Aerosol Size Distributions: Observations of Ultrafine Particles Events. Aerosol Science and Technology 34, 75-87.

ANNEX

Birmingham intercomparison

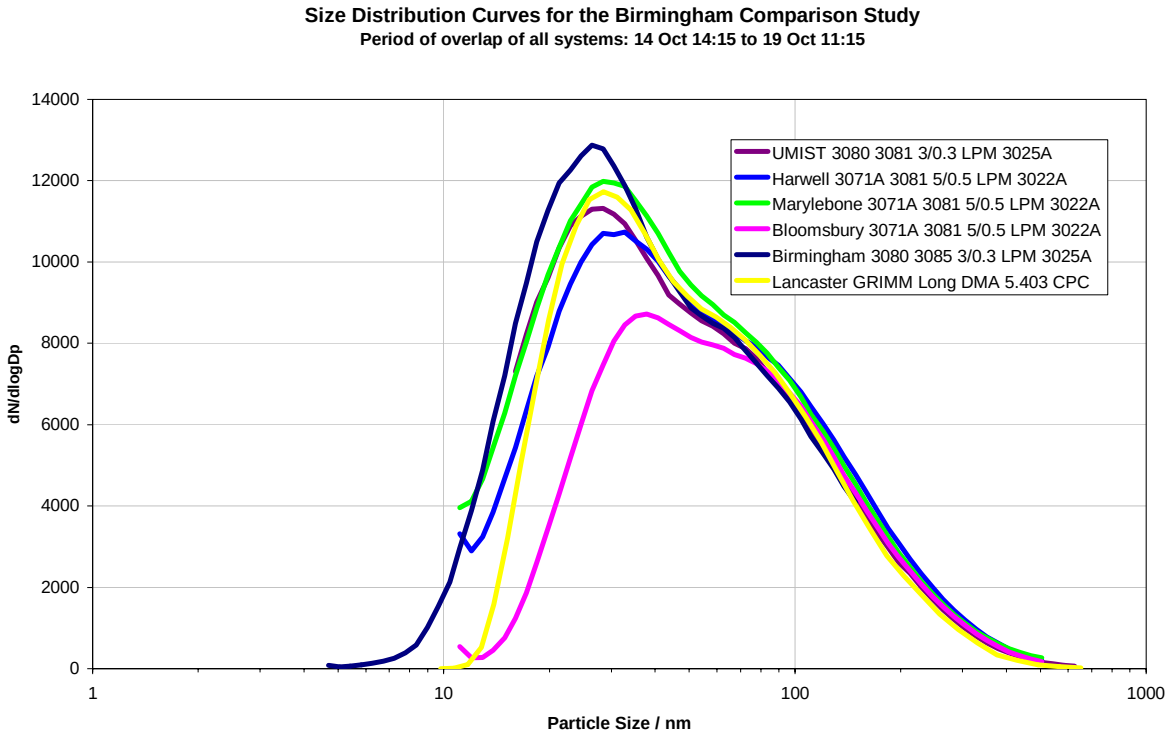

Figure 7 : Average particle number size distributions from 6 instruments including the Marylebone Road SMPS (green), the Bloomsbury SMPS (pink) and the Birmingham nano SMPS (dark blue)- data from David Harrison, Casella Stanger